US009819475B1

(12) **United States Patent**
Nessel et al.

(10) **Patent No.:** **US 9,819,475 B1**
(45) **Date of Patent:** **Nov. 14, 2017**

(54) WIRELESS NANOIONIC-BASED RADIO FREQUENCY SWITCH

(71) Applicants: **James A. Nessel**, Cleveland, OH (US); **Felix A Miranda**, Olmsted Falls, OH (US)

(72) Inventors: **James A. Nessel**, Cleveland, OH (US); **Felix A Miranda**, Olmsted Falls, OH (US)

(73) Assignee: **The United States of America as Represented by the Administrator of National Aeronautics and Space Administration**, Washington, DC (US)

(*) Notice: Subject to any disclaimer, the term of this patent is extended or adjusted under 35 U.S.C. 154(b) by 0 days.

(21) Appl. No.: **15/293,711**

(22) Filed: **Oct. 14, 2016**

Related U.S. Application Data

(63) Continuation of application No. 13/645,799, filed on Oct. 5, 2012, now Pat. No. 9,491,118.

(60) Provisional application No. 61/620,100, filed on Apr. 4, 2012.

(51) **Int. Cl.**
H04L 12/931 (2013.01)
H04L 5/14 (2006.01)
H04B 1/38 (2015.01)

(52) **U.S. Cl.**
CPC . ***H04L 5/14*** (2013.01); *H04B 1/38* (2013.01)

(58) **Field of Classification Search**
CPC H01L 45/1266
See application file for complete search history.

(56) **References Cited**

U.S. PATENT DOCUMENTS

7,923,715 B2	4/2011	Nessel et al.		
2010/0109656 A1*	5/2010	Wang	G01R 33/098	324/210
2010/0140582 A1*	6/2010	Nessel	H01L 45/00	257/4
2011/0269397 A1*	11/2011	Bella	H04B 7/15507	455/11.1
2011/0278528 A1*	11/2011	Lung	H01L 27/2454	257/2

OTHER PUBLICATIONS

Park, Ji-Yong, Han, Sang-Min, and Itoh, Tetsuo; "A Rectenna Design With Harmonic-Rejecting Circular-Sector Antenna"; IEEE Antennas and Wireless Propagation Letters, vol. 3, 2004.
McSpadden, James O., Fan, Lu, and Chang, Kai; Design and Experiments of a High-conversion-Efficienty 5.8-GHz Rectenna; IEEE Transactions on Microwave Theory and Techniques, vol. 46, No. 12, Dec. 1998, pp. 2053-2060.

(Continued)

Primary Examiner — Jay P Patel
(74) *Attorney, Agent, or Firm* — Robert H. Earp, III

(57) ABSTRACT

A nanoionic switch connected to one or more rectenna modules is disclosed. The rectenna module is configured to receive a wireless signal and apply a first bias to change a state of the nanoionic switch from a first state to a second state. The rectenna module can receive a second wireless signal and apply a second bias to change the nanoionic switch from the second state back to the first state. The first bias is generally opposite of the first bias. The rectenna module accordingly permits operation of the nanoionic switch without onboard power.

8 Claims, 17 Drawing Sheets

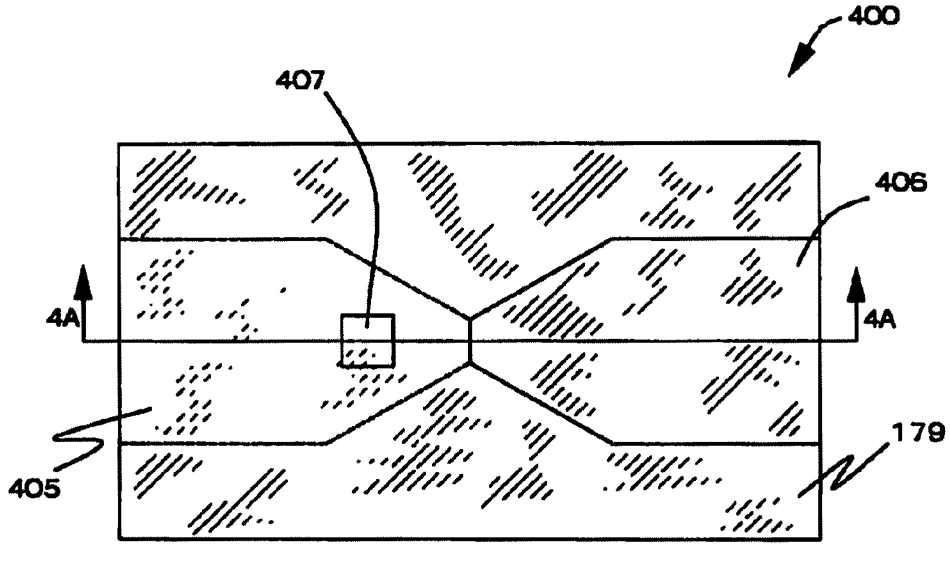

(56) References Cited

OTHER PUBLICATIONS

Nessel, James A., Lee, Richard O., Mueller, Carl H., Koxicki, Michael N., Ren, Minghan, and Morse, Jacki; "A Novel Nanoionics-based Switch for Microwave Applications"; IEEE 2008, 978-4244-1780-3/08/$25.00; pp. 1051-1054.
Yadav, Rakesh Kumar, Yadava, R. L., and Das, Sushrut; "The Rectennas—A progressive study"; ISSN: 2229-6646 (online) International Journal of Science Technology and Management (IJSTM), vol. 2 Issue 3, Jul. 2011 www.ijstm.com; pp. 119-126.

* cited by examiner

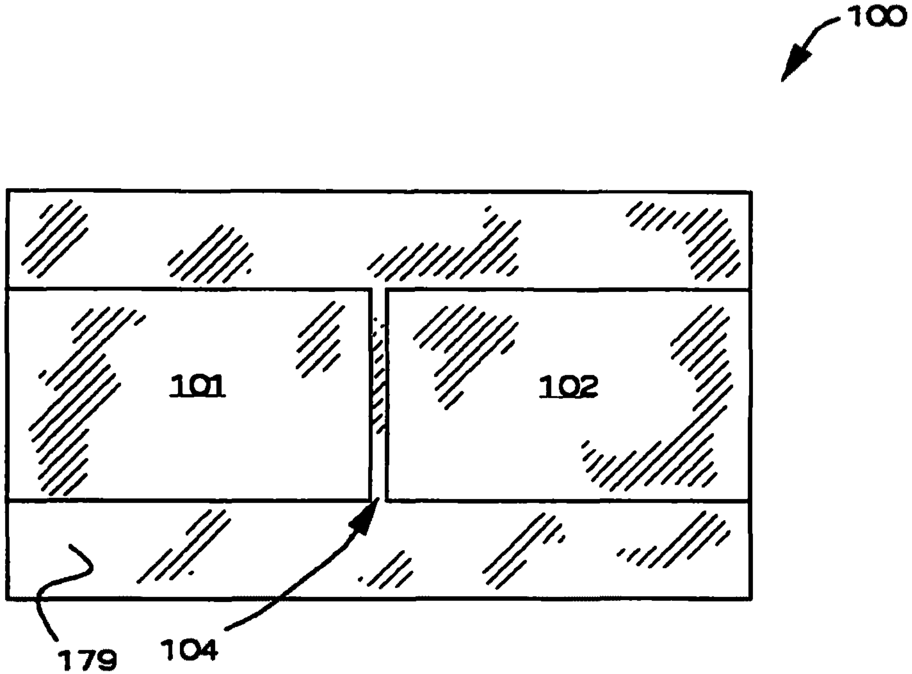
100
101
102
179
104

FIG. 1

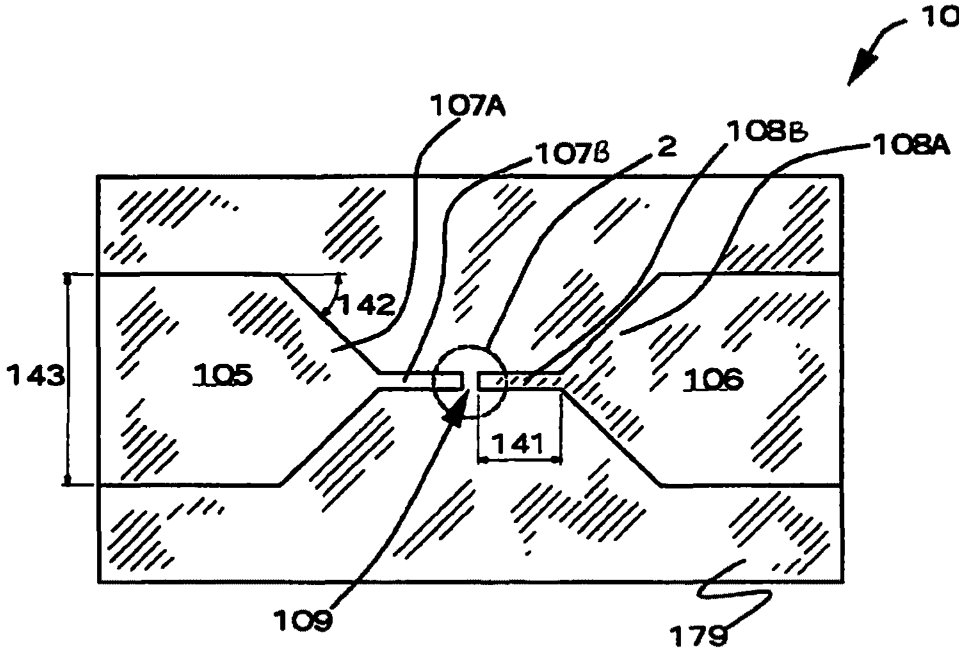
100A
107A
107B
2
108B
108A
142
143
105
106
141
109
179

FIG. 1A

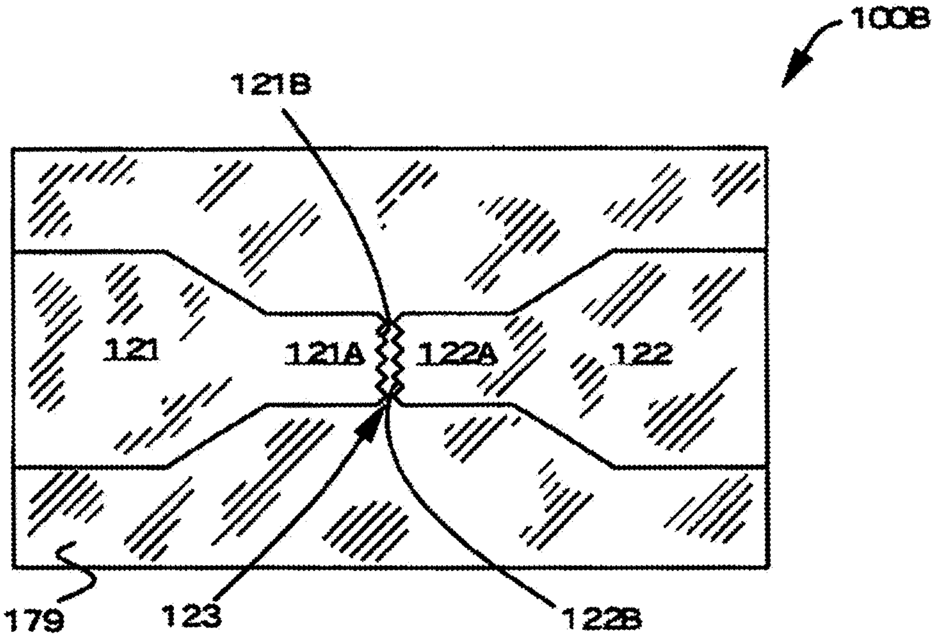
100B
121B
121
121A
122A
122
179
123
122B

FIG. 1B

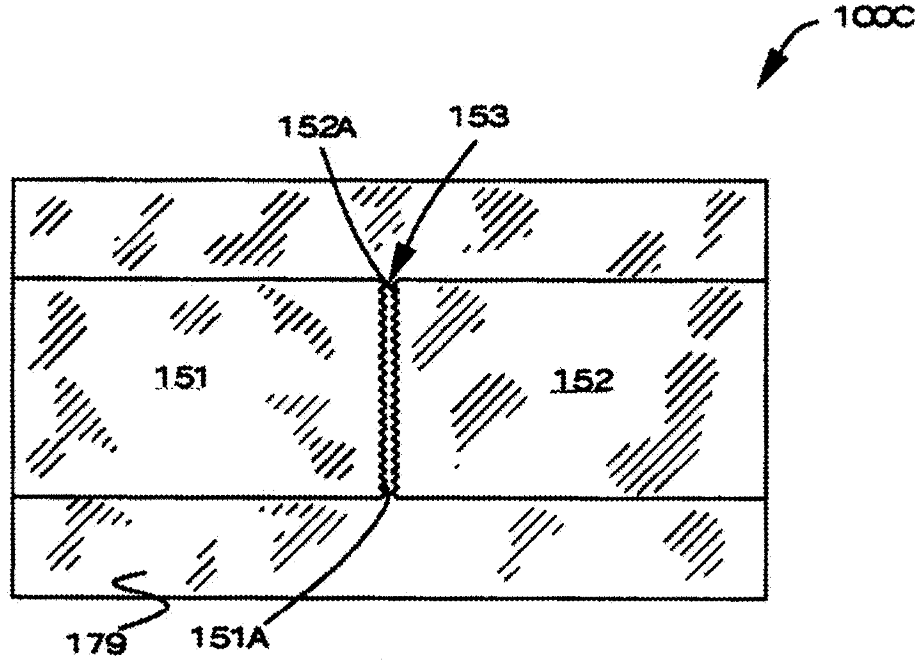
100C
152A
153
151
152
179
151A

FIG. 1C

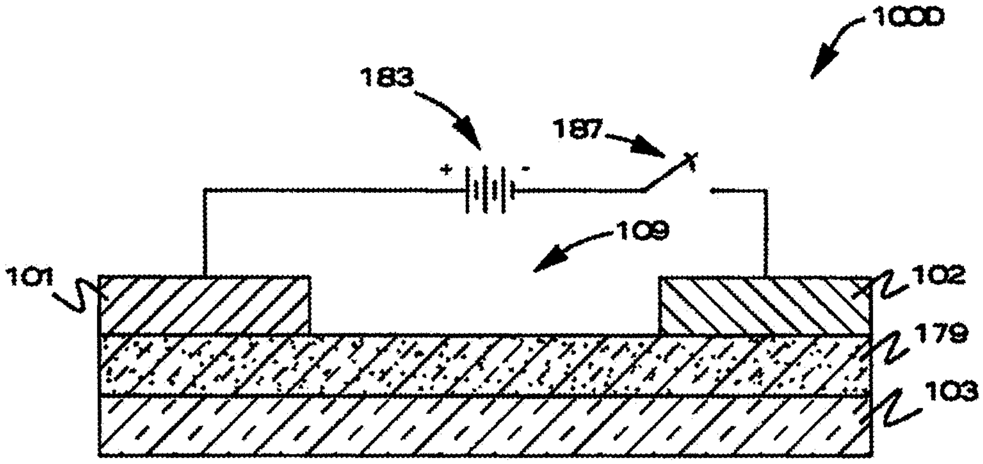
100D
183
+
-
187
109
101
102
179
103

FIG. 1D

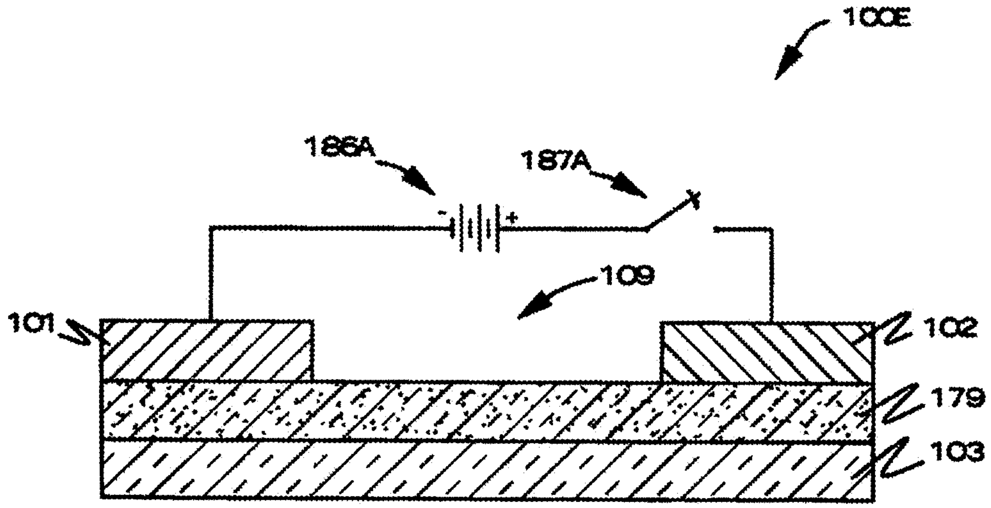
100E
186A
187A
-
+
109
101
102
179
103

FIG. 1E

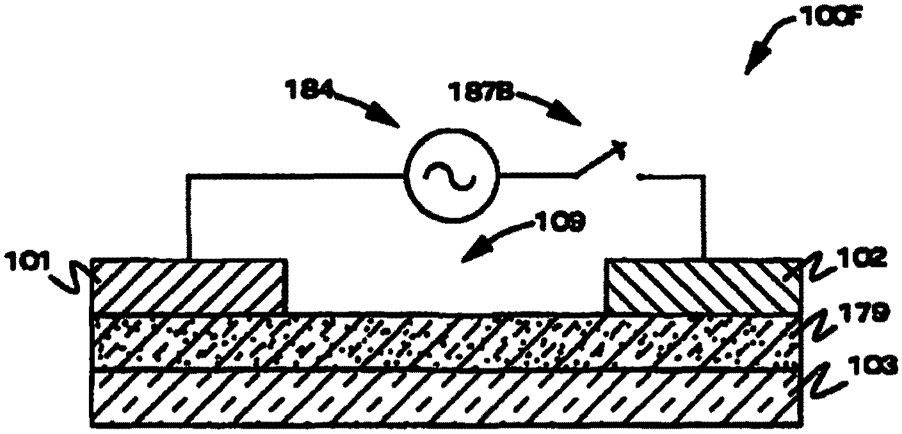

FIG. 1F

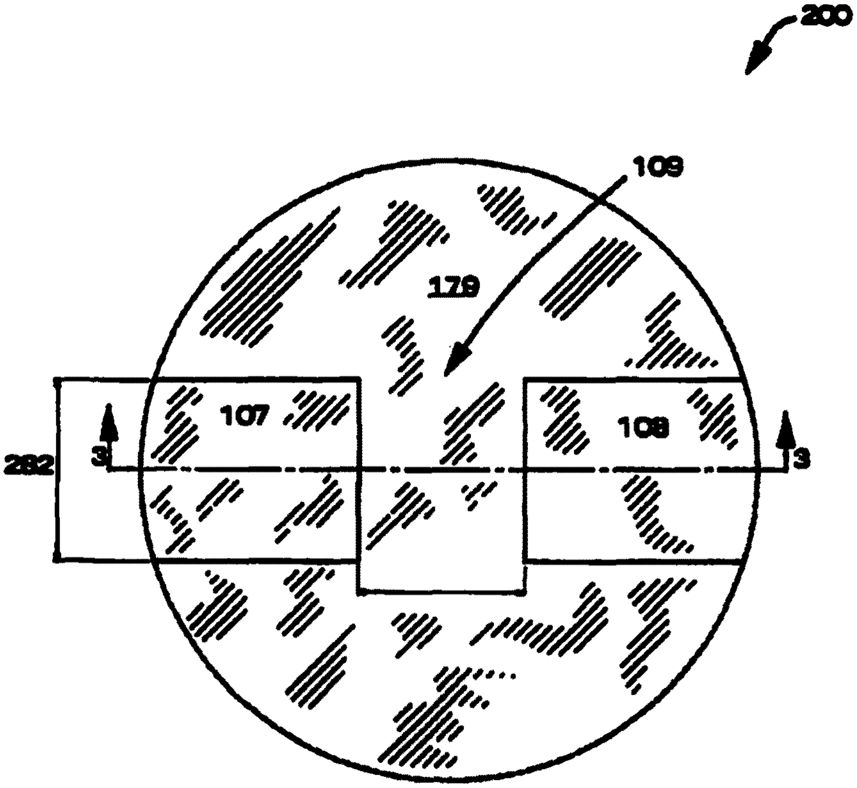

FIG. 2

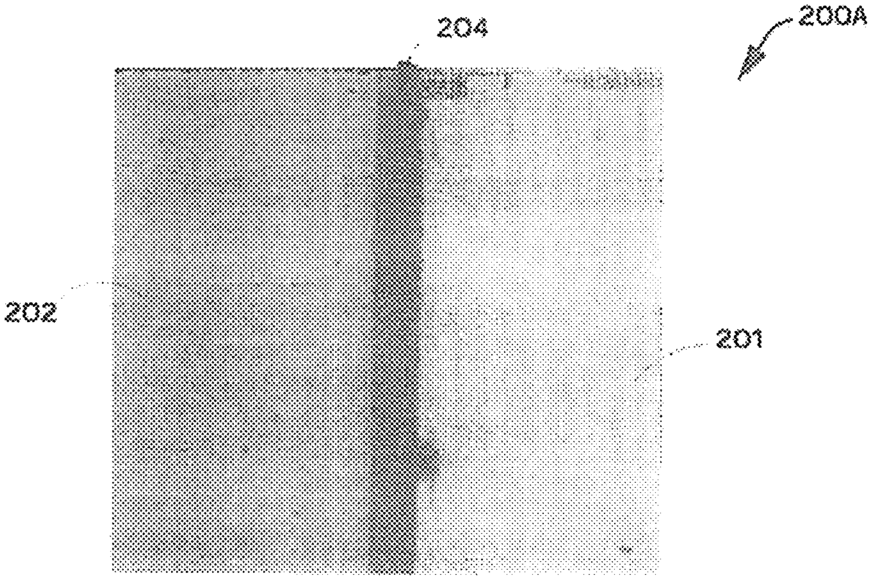

FIG. 2A

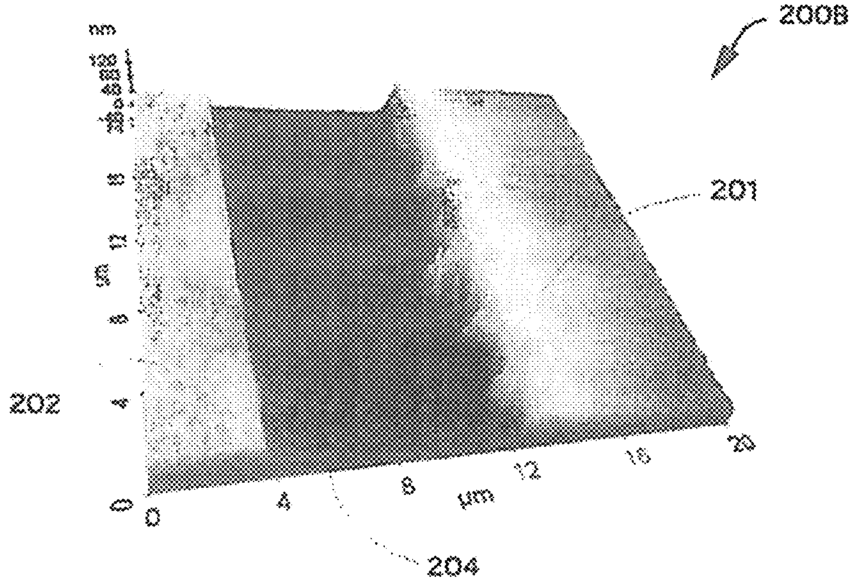

FIG. 2B

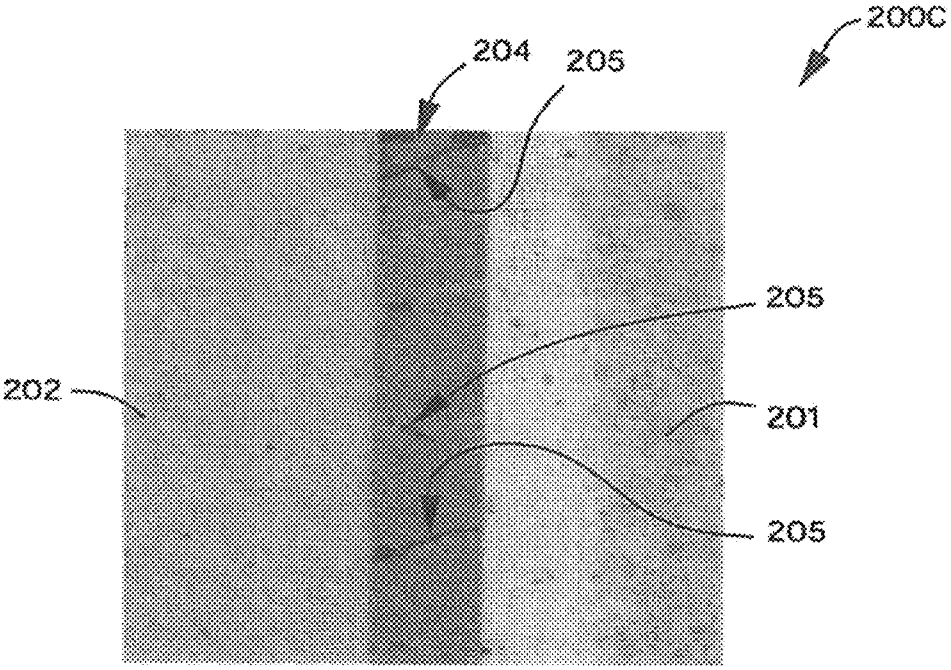
200C
204
205
205
202
201
205

FIG. 2C

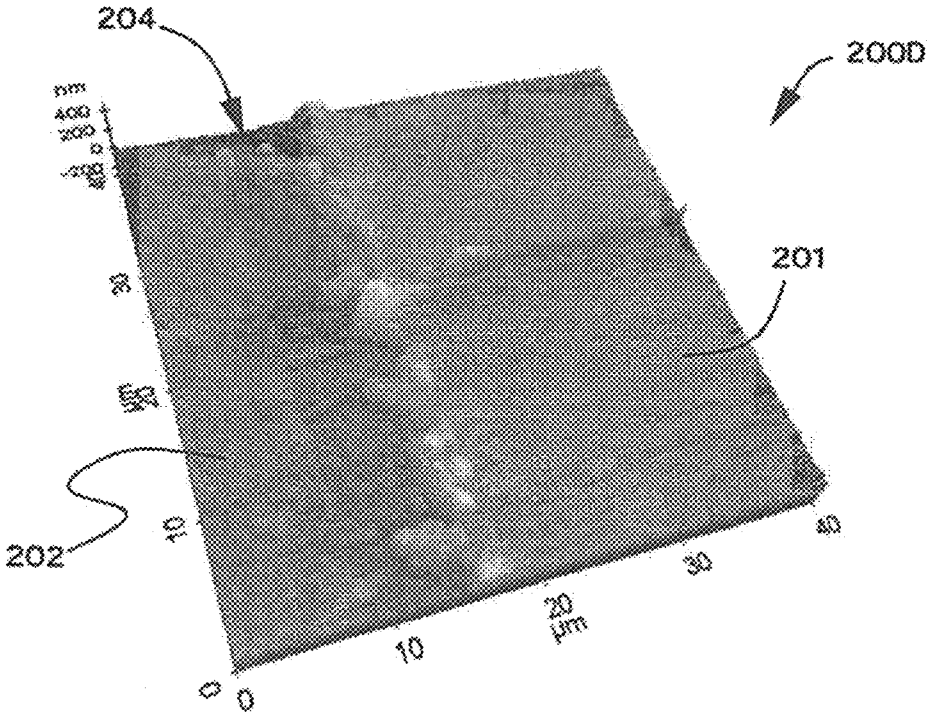
204
200D
nm
400
200
0
-200
30
µm 20
201
202
10
0
0
10
20 µm
30
40

FIG. 2D

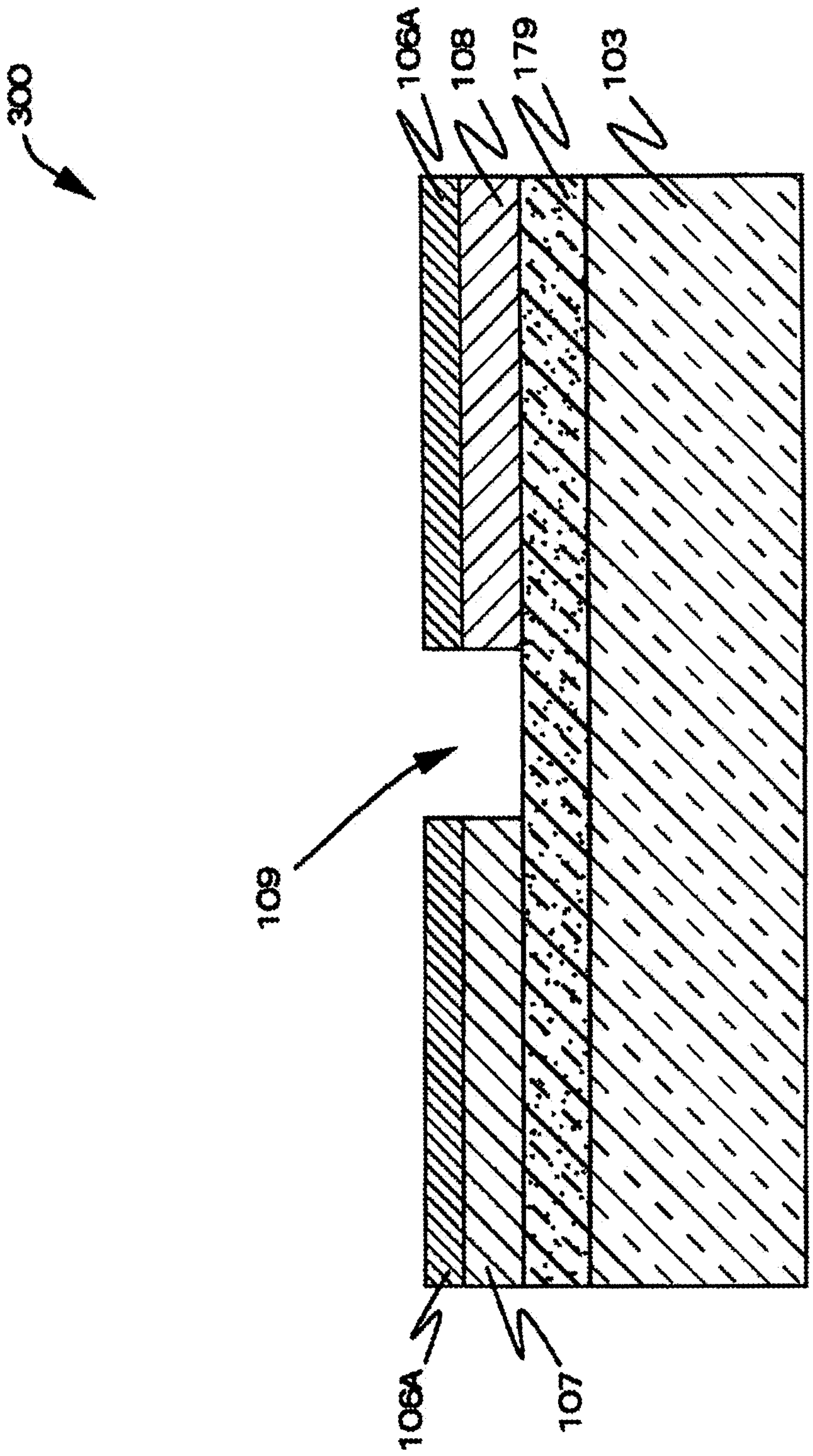

FIG. 3

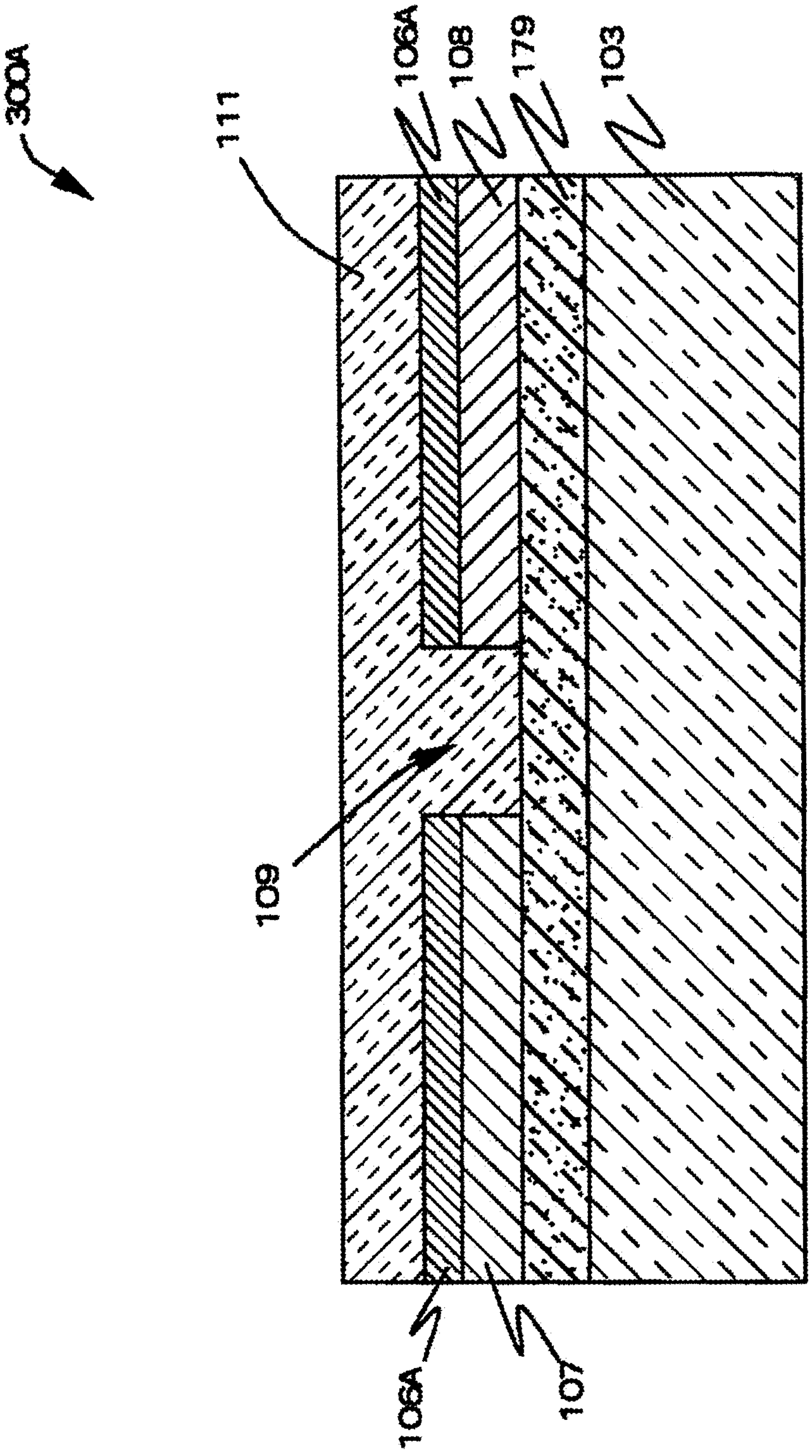

FIG. 3A

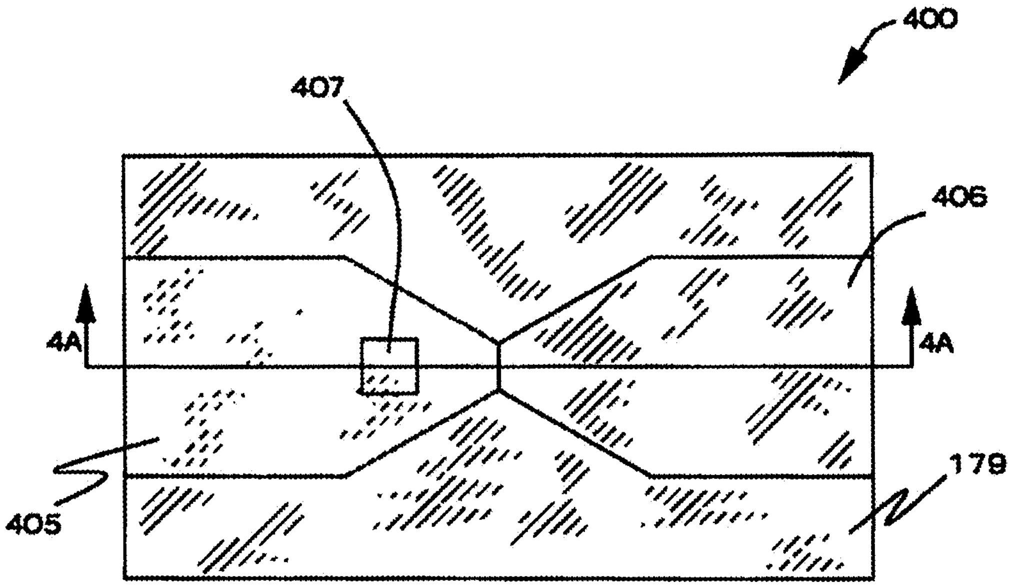

FIG. 4

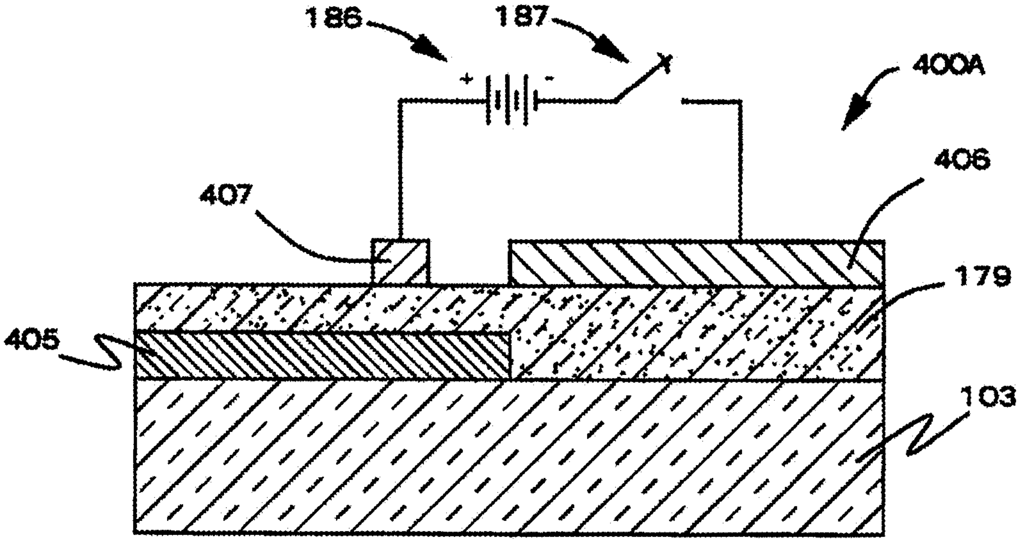

FIG. 4A

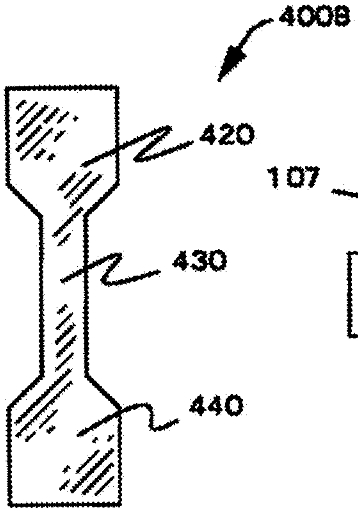

FIG. 4B

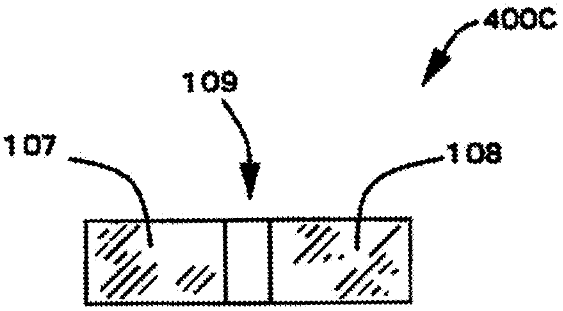

FIG. 4C

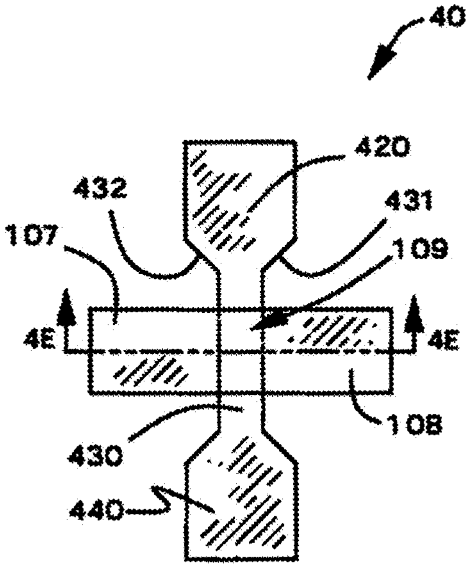

FIG. 4D

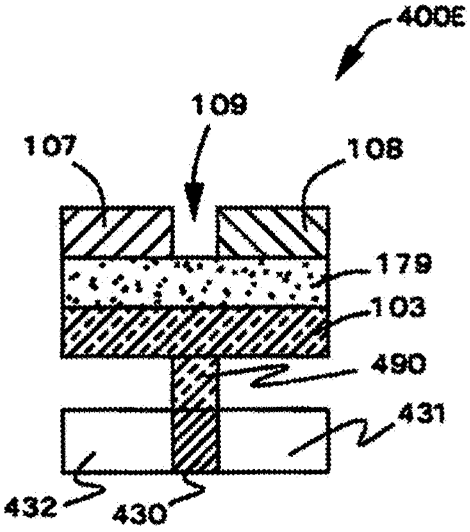

FIG. 4E

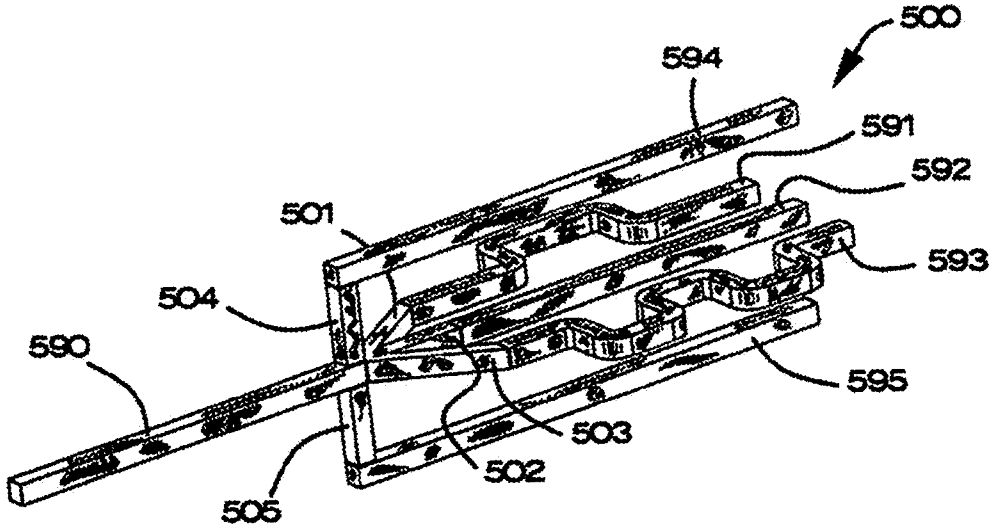
500
594
591
592
501
593
504
590
595
503
502
505

FIG. 5

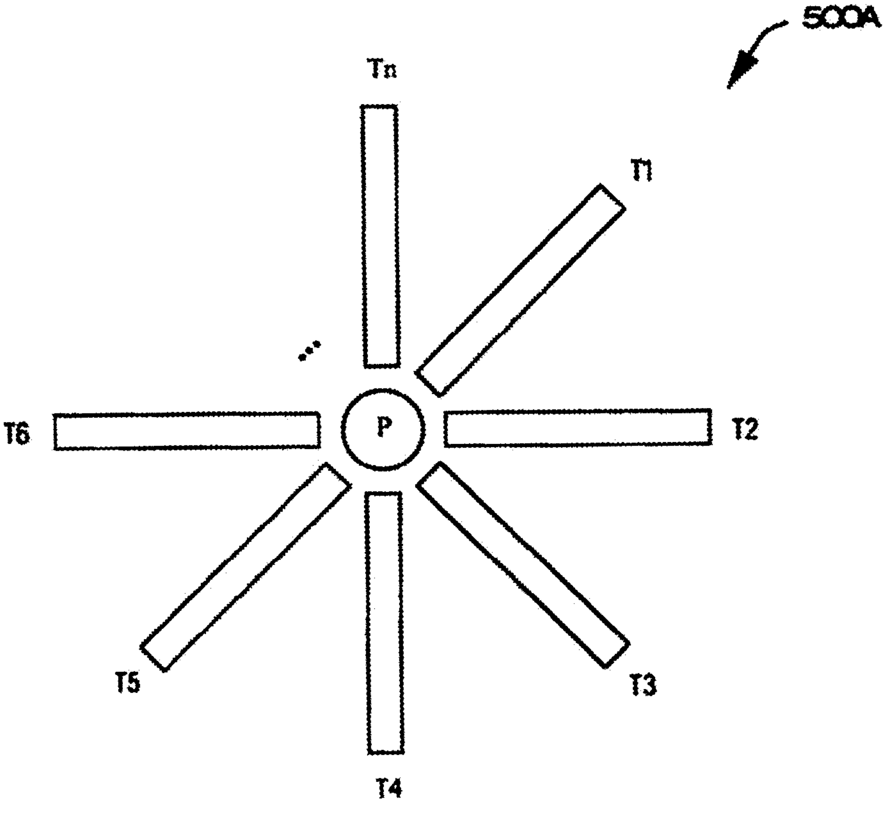
500A
Tn
T1
...
T6
P
T2
T5
T3
T4

FIG. 5A

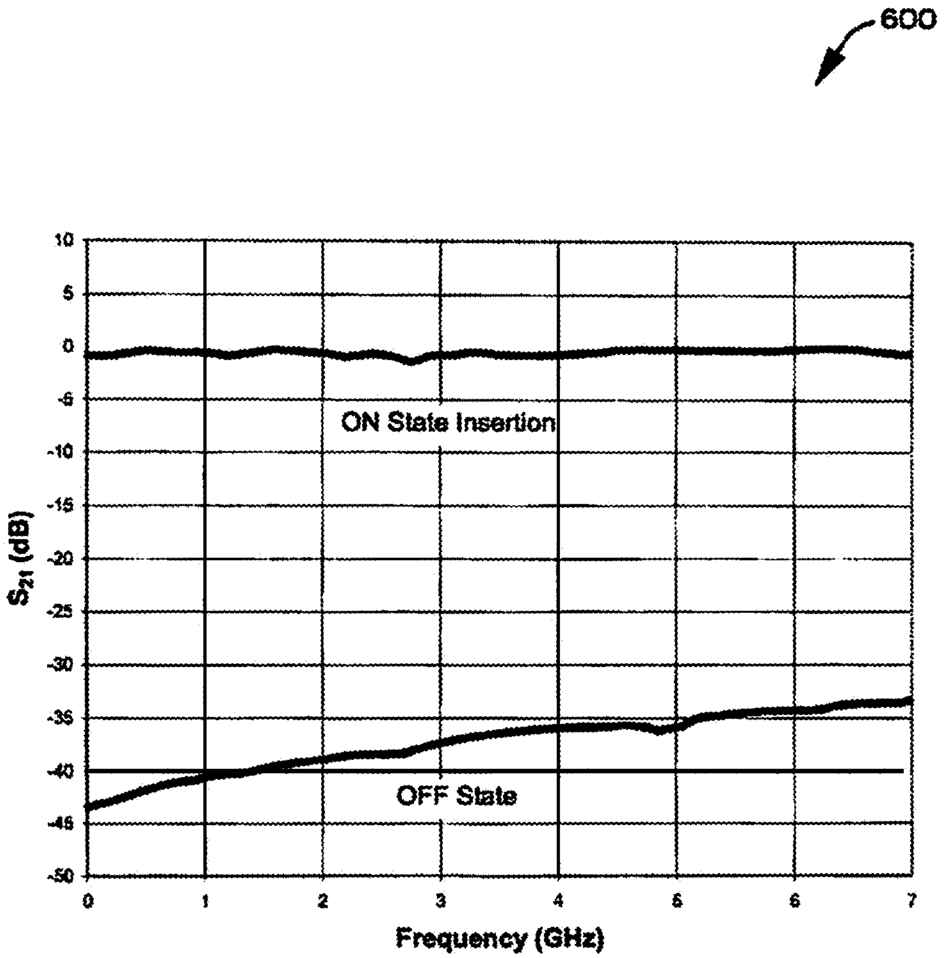
600
10
5
0
-5
-10
-15
-20
-25
-30
-35
-40
-45
-50
S_{21} (dB)
ON State Insertion
OFF State
0
1
2
3
4
5
6
7
Frequency (GHz)

FIG. 6

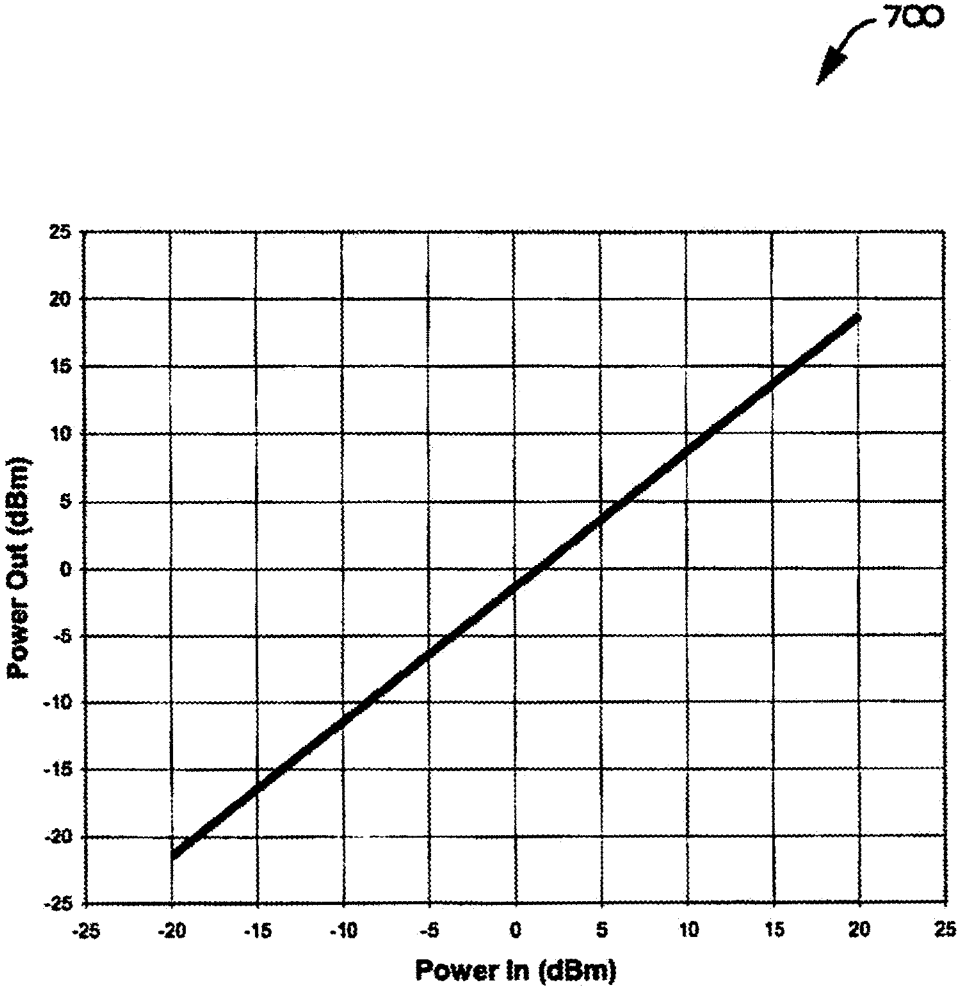
700
Power Out (dBm)
25
20
15
10
5
0
-5
-10
-15
-20
-25
-25
-20
-15
-10
-5
0
5
10
15
20
25
Power In (dBm)

FIG. 7

800

	MEMS	Solid State	Nanoionics
Frequency Range	DC to 70 GHz	DC to 20 GHz	DC to 6 GHz
Insertion Loss (avg)	0.1 dB	0.5 dB	0.5 dB
Isolation (avg)	40 dB	30 dB	35 dB
Actuation Voltage	5 - 50 V	3 - 5 V	1 V
Power Consumption	µW	mW	µW
Energy Consumption	0.1 – 10 µJ	µJ - mJ	100 nJ
Power Handling	1 - 20 W	1 - 10 W	0.5 W
Intermodulation Distortion	+80 dBm	+70 dBm	+75 dBm
Switching Speed	1 – 200 µs	10 - 100 ns	< 1 – 10 µs
Size	μm^2	$nm^2 – \mu m^2$	$nm^2 – \mu m^2$
Unit Cost	~ $5	~ $0.50	~ $0.50

FIG. 8

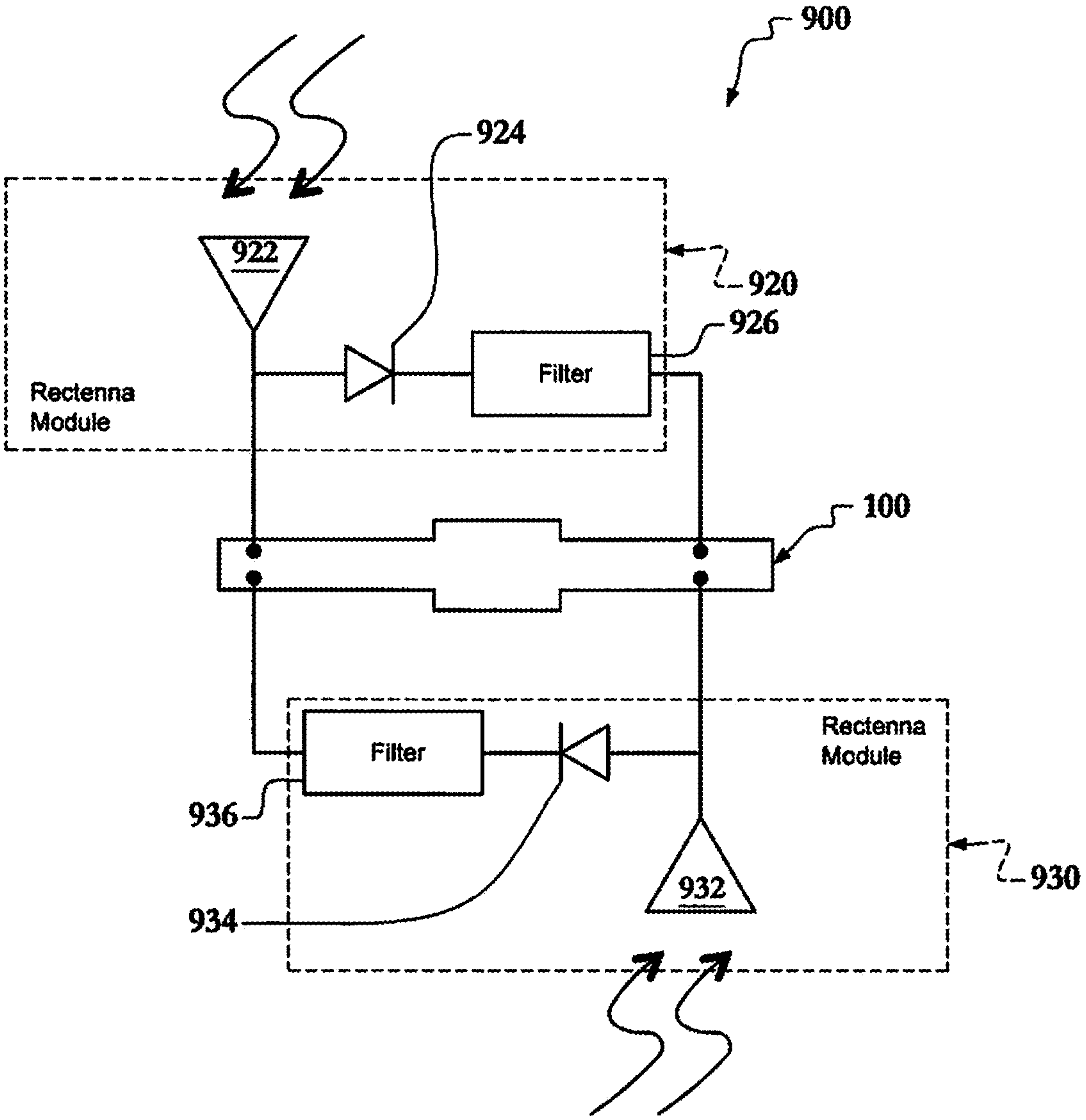
900
924
922
920
926
Filter
Rectenna Module
100
Rectenna Module
Filter
936
930
932
934

FIG. 9

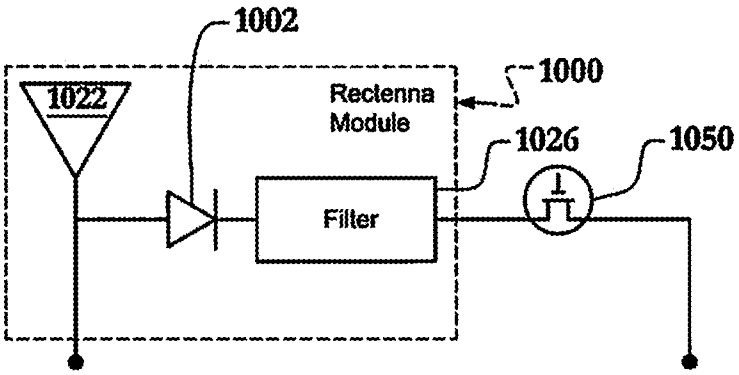

FIG. 10

WIRELESS NANOIONIC-BASED RADIO FREQUENCY SWITCH

CROSS REFERENCE TO RELATED APPLICATIONS

This application is a Continuation application claiming the benefit of priority from U.S. patent application Ser. No. 13/645,799, filed on Oct. 5, 2012, pending, which claims priority to U.S. Patent Application No. 61/620,100, entitled "Wireless Controlled Chalcogenide Nanoionic Radio Frequency Switch," filed on Apr. 4, 2012, each of which is hereby incorporated by reference in its entirety.

This application is related to U.S. Pat. No. 7,923,715, issued on Apr. 12, 2011, entitled "Chalcogenide Nanoionic-Based Radio Frequency Switch," is hereby incorporated by reference in its entirety, and is commonly assigned to the assignee of this application.

STATEMENT REGARDING FEDERALLY SPONSORED RESEARCH OR DEVELOPMENT

The invention described herein was made by an employee of the United States Government and may be manufactured and used by or for the Government for Government purposes without the payment of any royalties thereon or therefore.

BACKGROUND OF THE DISCLOSURE

Radio frequency switches are basic building blocks for communication and control systems and are used for multiplexing of signals to achieve system reconfigureability and dynamic control. Radio frequency switches may be used in such applications as portable/mobile/satellite communication systems (e.g. cell-phones, PDAs, laptops, phased array antennas, sensors, transceivers etc.). As communication systems approach higher data rate (gigabytes per second) and multi-functional operation, stringent requirements have been set for radio frequency switches. Some of these requirements include low power consumption, high reliability, high switching speed, high isolation, low insertion losses, ease of integration/implementation, as well as affordability. In particular, for 3G (third generation) wireless phones and space-based applications, low power consumption is critical to ensure reliable, long lifetime operation on limited power supplies. MEMS or solid-state based switches which are currently used are incapable of meeting future demands due to associated disadvantages. For example, MEMS devices utilize complicated manufacturing processes and are expensive to manufacture. FIG. **8** is a table comparing electronic, physical and cost properties of MEMS, solid state, and nanoionic switches.

Known radio frequency devices employ electronic, mechanical, or a combination of electronic and mechanical (electromechanical) processes to induce a change in state (on/off). Radio frequency switching applications usually employ solid state switches or microelectromechanical systems (MEMS), both of which possess associated weaknesses. Solid state diodes can be produced cost-effectively to operate at low voltages (1-3V) and high speeds (ns), but suffer from higher insertion loss, high DC power consumption, low isolation, and the generation of third-order harmonics/intermodulation distortion (IMD). MEMS-based switches provide low insertion loss (about 0.2 dB), low DC power consumption (about pW), high isolation (>30 dB), and good IMD performance, but exhibit reliability problems (e.g., stiction, moving parts), slower switching speeds (μs), high actuation voltages (5-50V) which require complex circuitry, and relatively complicated processing steps. Furthermore, MEMS packaging presents additional problems which need to be addressed before widespread use is realizable.

Advances in the area of radio frequency switches will be beneficial in various industries. The present disclosure addresses embodiments that may be applicable to switches, such as radio switches.

SUMMARY OF THE INVENTION

A method of wirelessly transmitting a first signal at a first frequency is disclosed herein. The method includes receiving the signal at a first antenna and applying a first bias based on the first signal across a nano-ionic switch. The first bias changes a state of the nano-ionic switch from a first state to a second state.

A method comprising wirelessly transmitting a signal at a first frequency is disclosed. The method includes receiving the signal at a rectenna module and converting the signal to electrical current at the rectenna module. The method further includes directing the electrical current to a nano-ionic switch wherein the electrical current changes a state of the nano-ionic switch from a first state to a second state or vice versa.

A system is also disclosed comprising a rectenna module having an antenna and a rectifier configured to receive a first radio wave signal at a first frequency and convert the radio wave signal into electrical current. The system can also include a nano-ionic switch connected to the rectenna module. The nano-ionic switch has an oxidizable electrode and an inert electrode positioned on chalcogenide glass such that a gap exists between the oxidizable electrode and the inert electrode. Receipt of the current at the nano-ionic switch causes the oxidizable electrode and the inert electrode form a conductive bridge at the gap without any power source.

BRIEF DESCRIPTION OF THE DRAWINGS

FIG. **1** is a schematic top view of a first example of a nanoionic switch.

FIG. **1**A is a schematic top view of a second example of a nanoionic switch that illustrates electrodes with a gap therebetween.

FIG. **1**B is a schematic top view of a third example of a nanoionic switch that illustrates electrodes with serrated edges opposed from one another.

FIG. **1**C is a schematic top view of a fourth example of a nanoionic switch that illustrates electrodes with serrated edges of a higher frequency than that of FIG. **1**B.

FIG. **1**D is a schematic cross-sectional view of a substrate, solid electrolyte, electrodes and a direct current voltage source.

FIG. **1**E is a schematic cross-sectional view of a substrate, solid electrolyte, electrodes and a direct current voltage source having an opposite bias from that of FIG. **1**D.

FIG. **1**F is a schematic cross-sectional view of a substrate, solid electrolyte, electrodes, switch and an alternating voltage source.

FIG. **2** is an enlargement of a portion of FIG. **1**A illustrating a gap between the electrodes.

FIG. **2**A is a microphotograph of a portion of an oxidizable electrode, an inert electrode and a gap of a nanoionic switch (depicted schematically in FIG. **1**) in the "off" state (switch is open).

FIG. **2**B is an atomic force microscopic image of a portion of a gap and electrodes of the actual nanoionic switch of FIG. **2**A (depicted schematically in FIG. **1**) with the switch in the "off" state (switch is open).

FIG. **2**C is a microphotograph of a portion of an oxidizable electrode, inert electrode and a gap therebetween of the nanoionic switch depicted schematically in FIG. **1** in the "on" state (switch is closed).

FIG. **2**D is an atomic force microscopic image of a portion of the gap and electrodes of a nanoionic switch of FIG. **2**C depicted schematically in FIG. **1** in the "on" state (switch is closed).

FIG. **3** is a schematic cross-sectional view taken along the lines **3**-**3** of FIG. **2** illustrating a substrate, a chalcogenide glass layer, and metallic plated electrodes.

FIG. **3**A is schematic cross-sectional view illustrating the substrate, the metallic plated electrodes and a passivation layer above the electrodes and traversing the gap between the electrodes.

FIG. **4** is schematic top view of a nanoionic capacitor.

FIG. **4**A is a schematic cross-sectional view of the nanoionic capacitor of FIG. **4** illustrating electrodes.

FIG. **4**B is a top schematic view of a lower plate of a nanoionic capacitor.

FIG. **4**C is a top schematic view of a nanoionic switch that forms one of the two capacitor plates of the example of the nanoionic capacitor schematically illustrated in FIGS. **4**B-**4**E.

FIG. **4**D is a top schematic view of the capacitor plates illustrated in the overlapping position crossing each other in an orthogonal relationship.

FIG. **4**E is a cross-sectional view of the nanoionic capacitor of FIG. **4**D taken along the lines **4**E-**4**E.

FIG. **5** is a schematic of a vertical and horizontal switch to various lines having different lengths to accommodate phase shifting.

FIG. **5**A is a schematic of a single pole "N" throw nanoionic switch.

FIG. **6** is a plot of insertion loss (switch closed or "on") and the isolation (switch open or "off") for frequencies between 1 and 6 Ghz.

FIG. **7** is a generalized plot of power in versus power out for four frequencies (500 MHZ, 1 GHz, 2 GHz and 4 GHz).

FIG. **8** is a table comparing electronic, physical and cost properties of MEMS, solid state, and nanoionics switches.

FIG. **9** illustrates a first rectenna module and a second rectenna module electrically connected to a nano-ionic switch in an embodiment of the disclosure.

FIG. **10** illustrates a rectenna module and a polarity switch electrically connected in an embodiment of the disclosure.

DESCRIPTION OF EMBODIMENTS OF THE DISCLOSURE

The present disclosure sets forth embodiments as examples of those inventions set forth in the claims section. More specifically, the present disclosure relates to a nanoionic switch that may be used in various applications. No term or phrase in the Description section is meant to limit any claim term unless specifically set forth in the claims section. Those having ordinary skill in the art will appreciate alternatives to the disclosure set forth herein are possible without departing from the inventive concepts contained herein.

The fundamental operation of the nanoionic switch is rooted in the phenomenon of ion conduction in solid electrolytes. Comparable to liquid electrolytes (e.g., lead-acid batteries), solid electrolytes consist of mobile ions which undergo oxidation/reduction reactions at the anode (oxidizable electrode) and cathode (inert electrode) of the system. The fundamental difference between solid electrolyte and liquid electrolyte behavior is that the mobile ions are of a single polarity while the opposite polarity species remain fixed. The fixed ions essentially create a solid matrix in which mobile ions can "hop" into neighboring potential wells. Based on this short-range hopping mechanism for conduction, the ionic conductivity of solid electrolytes can approach electronic conductivity levels in semiconductors. See, "Devices Based on Mass Transport in Solid Electrolytes," Michael N. Kozicki and Maria Mitkova, Center for Applied Nanoionics, Arizona State University. Advantageously, the electrochemical resistance-change process may be performed with minimal energy.

FIG. **1** is a schematic view of a first example of a nanoionic switch **100**. The fabrication of the nanoionics-based switch **100** can include a substrate **103**, as shown in FIGS. **1**D and **1**E. The substrate **103** can have a relatively high resistivity, such as a silicon wafer or other substance with a relatively high resistance, such as a resistance greater than 1000 Ohm per centimeter. A base material **179** may be positioned on the substrate **103**. The base material **179** may comprise one or more layers, or a ternary. In an embodiment, the base material **179** includes a layer of a glass material, such as chalcogenide glass.

Many inorganic and organic materials could be used as the base material **179** to conduct ions to at least some extent. Compounds of elements in the column of the periodic table headed by oxygen, the so-called chalcogens, are useful in electrochemical switching devices and/or the switch **100**. Chalcogens can be used because of their high ion availability and mobility at normal device operating temperatures. As an embodiment, the chalcogenide glass may be utilized as the base material **179**. For example, the chalcogenide glass can comprise a binary chalcogenide glass utilizing elements in column IV and/or VI of the periodic table, including but not limited to germanium, selenium, sulfur, silicon, oxygen amongst the other elements in those columns and other elements having similar properties for the given application. Stable binary glasses typically involve a group IV or group V atom, which non-limiting examples of the binary chalcogenide glass include but are not limited to germanium-selenium, germanium-sulfur, silicon-oxygen. In an embodiment where germanium and selenium are used, the germanium and selenium content of the binary may range from 30 to 40 percent by weight. Non-oxide glasses are more rigid than organic polymers but more flexible than a typical oxide glass. The flexibility of these materials offers the possibility of the formation of voids through which the ions can readily move from one equilibrium position to another.

Electrodes may be formed at opposing ends of the base material **179** whereby ions from at least one of the electrodes is capable of moving toward the other electrode. For example, a first electrode **101**, a second electrode **102** and a gap **104** therebetween are illustrated in FIG. **1**. In the embodiment of FIG. **1**, the gap **104** can have a length of approximately 10 micrometers (μm). Of course, the size of the gap **104** may be any size as required by the nanoionic switch **100**. The first electrode **101** may be an oxidizable electrode and may be positioned adjacent one end of the base material **179**. The second electrode **102** may be an inert electrode and may be positioned adjacent an opposite end of the base material **179** such that the gap **104** is formed between the first electrode **101** and the second electrode **102**.

The base material **179** may be positioned between the substrate **103** and the electrodes **101**, **102**.

The first electrode **101** and the second electrode **102** may have one or more metallic layers, which can be deposited atop the base material **179**. Dissimilar metals can be used for the electrodes **101**, **102**. For example, the first electrode **101** may be an oxidizable metal, such as silver, and the second electrode **102** may be an inert metal, such as tungsten or nickel. A person having ordinary skill in the art will appreciate that the present disclosure may utilize other materials for the substrate **103**, the base material **179** and the electrodes **101**, **102**. In an embodiment, the switch **100** includes a passivation layer to protect the layers of the switch **100** from the environment.

When a metal ion is introduced into the chalcogenide glass, the ions nucleate on the chalcogen-rich regions within the chalcogenide glass, resulting in a ternary that takes the form of a dispersed nanoscale metal ion-rich phase in a continuous glassy matrix. This allows the electrolyte to have a relatively high resistivity (necessary for a high off resistance state), while containing large quantities of highly mobile metal ions for conduction.

As a non-limiting example, "[t]he addition of Ag (or Cu) to the chalcogenide base glass can be achieved by diffusing the mobile metal from a thin surface film via photo dissolution. The process utilizes light energy greater than the optical gap of the chalcogenide glass to create charged defects near the interface between the reacted and unreacted chalcogenide layers. The holes created are trapped by the metal while the electrons move into the chalcogenide film. The electric field formed by the negatively charged chalcogen atoms and positively charged metal ions is sufficient to allow the ions to overcome the energy barrier at the interface and so the metal moves into the chalcogenide. Prior to the introduction of the metal, the glass consists of GeS_4 tetrahedra and, in the case of chalcogen-rich material, S (Se) chains. The introduced metal will readily react with the chain chalcogen and some of the tetrahedral material to form the ternary. This Ag chalcogen reaction, which essentially nucleates on the chalcogen-rich regions within the base glass, results in the nanoscale phase-separated ternary." See, "Devices Based on Mass Transport in Solid Electrolytes," Michael N. Kozicki and Maria Mitkova, Center for Applied Nanoionics, Arizona State University.

In an embodiment, the electrodes **101**, **102** are approximately 1.5-2 μm thick and the base material **179** is approximately 100 nm thick. The base layer **179** is illustrated as applied to the substrate **103**. In an embodiment where silver is used as a metallic layer, appropriate amounts and thicknesses of silver film is used such that the photodissolution of the silver will completely saturate the base material **179**. In other words, the base material **179** of FIG. **1** is completely saturated.

FIG. **1**A is a schematic top view of a second example of a nanoionic switch **100**A which illustrates narrow portions **107**B, **108**B of electrodes **105**, **106**. The electrode **105**, **106** may be or the electrodes **101**, **102** or have similar structure to the electrodes **101**, **102**. In an embodiment, the electrode **105** is a silver electrode (oxidizable), and the electrode **106** is the nickel (inert) electrode. In the embodiment shown, a width **143** of the electrodes **105**, **106** can be approximately 1 millimeter (mm). The electrodes **105**, **106** may include tapered portions **107**A, **108**A which may be tapered at an angle **142**, as shown in FIG. **1**A. The angle **142** may be less than 90 degrees, such as less than 45 degrees, including approximately 225 degrees as shown in FIG. **1**A. The tapered portions **107**A, **108**A may extend toward elongated narrow portions **107**B, **108**B. For example, in an embodiment, a length **141** of the elongated narrow portions **107**B, **108**B as shown in FIG. **1**A may be approximately 50 μm. Further, in this embodiment, a width of the narrow portions **107**B, **108**B may be approximately 10 μm, but a person having ordinary skill in the art will appreciate various dimensions of the narrow portions **107**B, **108**B may be utilized effectively. As a non-limiting example, the narrow portions **107**B, **108**B may be equal or less than 10 μm wide, and, in an embodiment, the width may range from 2-10 μm. The angle **142**, the width **143** of the electrodes **105**, **106**, and the length and width of the elongated extensions **107**, **108** can be sized as will be required by the application of the switch **100**. For example, the size of the electrodes **105**, **106** and/or the elongated extension **107**, **108** can be configured for frequency operation in the range of 1 MHz to 6 GHz. Other considerably different geometries may be used without departing from the spirit and the scope of the disclosure as set forth herein for frequencies of operation outside the range specified herein.

A gap **109** may be positioned between the elongated narrow portions **107**B, **108**B. For example, the elongated narrow portion **107**B, **108**B may extend toward each other but terminate such that the gap **109** is formed therebetween. The gap **109** may be approximately 10 μm, in one such embodiment, for example. FIG. **2** is an enlargement of a portion **200** of FIG. **1**A illustrating the gap **109** between the electrodes **107**, **108**. The width **282** of the gap **109** is shown in FIG. **2**.

The electrodes **105**, **106**, the tapered portions **107**A, **108**A thereof and the elongated narrow extensions **107**B, **108**B thereof may be metallic plated **106**A, such as gold plated. Reference numeral **106**A is used in FIGS. **3** and **3**A to illustrate the metallic plating (for example, coating) of the electrodes **105**, **106**. It should be noted that the electrodes **101**, **102** in FIGS. **1**A, **1**B and **1**C, may have metallic plating even though such embodiments are not illustrated as such, for the sake of clarity.

FIG. **1**B is a schematic top view of a third example of a nanoionic switch **100**B which illustrates electrodes **121**, **122** having serrated edges **121**B, **122**B opposed from one another. It will be noted that the serrations of the serrated edges **121**B, **122**B are matched peak to peak such that the smallest gap **123** is created between peaks and the gap being slightly larger from valley to valley. Still referring to FIG. **1**B, the oxidizable electrode **121** and the inert electrode **122** are illustrated. Tapered portions are illustrated as extending to elongated extensions **121**A, **122**A.

FIG. **1**C is a schematic top view of a fourth example of a nanoionic switch **100**C which illustrates electrodes **151**, **152** having serrated edges **151**A, **152**A of a higher frequency than that shown in FIG. **1**B. The serrated edges **151**A and **152**A indicate a minimum gap **153** at the peaks thereof as opposed from one another. Further, the electrode **151** can be an oxidizable electrode and the electrode **152** can be an inert electrode. In this embodiment, the electrode **151** may be silver, and the electrode **152** may be nickel. As in the examples illustrated in FIGS. **1**, **1**A, and **1**B, the electrodes **151**, **152** can be positioned on the base material **179**, such as a chalcogenide glass ternary, which may be doped with a metal, such as silver. For example, doping the chalcogenide ternary with metal, such as silver may be performed via photo-dissolution as discussed herein.

Electrolytes can be formed in a two-step process in which the base material **179**, such as the chalcogenide glass can be deposited onto the substrate **103**. Next, a metallic film is applied thereto. Then, as one example of how to migrate the metallic ions into the base material **179**, such as the glass matrix of the chalcogenide ternary, the metal may deposited atop the glass matrix and exposed to light to induce a photo-dissolution process, such as by utilizing ultraviolet light. The metallic ions can then migrate into the glass matrix providing the framework for ionic transport and the capability of switching between states, such as a low-loss "on" state and a high isolation "off" state. The glass deposition can be evaporated in a vacuum performed at or near room temperature, for example.

As one non-limiting example of the photo-dissolution process that may be used for the nanoionic switch **100**, **100**A, **100**B, **100**C, an ultraviolet source may be applied for a period of time. As an example, the ultraviolet source may have a wavelength of about 405 nanometers (nm) and a power density of approximately 5 mW/cm^2 and may be applied for a predetermined amount of time, such as about ten minutes. The metallic film thickness may be such that sufficient light can penetrate to the interface to stimulate the photo-dissolution process in a reasonable time. For example, the metallic film thickness can be less than 25 nm to permit the photo-dissolution process in a reasonable time, but may be adjusted as needed. "Saturation" of the base material **179** in an embodiment where the base material **179** is the chalcogenide glass ternary set forth herein can occur when the diffusing metallic film reacts with substantially, if not all, of the available chalcogen atoms. Accordingly, the amount of metallic film at saturation can depend on the amount of chalcogen of the base material **179**. As a non-limiting example, a 20 nm thick metallic film can completely saturate a 50 nm thick base material **179** when the photo-dissolution is completed. "Sub-saturated" electrolytes support electro-deposition but growth rates are typically reduced as there is less metal available. Electrolyte films as thin as 10 nm can be used for surface electro-deposition. Metallic deposition may also be performed using evaporation without breaking vacuum so as to prevent the formation of an oxide diffusion barrier on the surface of the glass. The thicknesses of both layers will largely depend on device performance requirements.

A representative nanoionic switch **100** can be seen in the microphotographs and atomic force photographs of FIGS. **2**A, **2**B, **2**C and **2**D. The photographs correspond to the example of FIG. **1**. Referring to FIGS. **2**A and **2**B, which are photomicrographs and atomic force photos, respectively, of a nano-ionic switch **200**A, **200**B, a chalcogenide ternary **204** is 100 nm thick and an oxidizable electrode **201** and an inert electrode **202** are approximately 2 μm thick. Accordingly, the chalcogenide ternary **204** is much thinner than the electrodes **201**, **202**.

For an ion current to flow in an electrolyte, the oxidizable electrode **201** is made positive (anode) with respect to the inert electrode **202** and sufficient bias is applied, typically on the order of a few tenths of a volt or more. As an example, for Ag^+ saturated $GeSe_2$, the oxidizable electrode **201** is oxidized to form an excess of Ag+ ions within the chalcogenide base glass. The applied field causes the silver positive ions to flow toward the inert electrode **202** through the coordinated hopping mechanism described above. At the inert electrode **202**, a reduction reaction occurs by injecting electrons to re-form the metal, such as silver metal. The number of atoms electrodeposited by the reduction of ions will correspond to the number of electrons that participate in the process (supplied by the external circuit, for example a voltage source or some other electronic component). The electrons are supplied by the direct current or alternating current voltage source. Each metal ion undergoing reduction will be balanced by a metal atom becoming oxidized to avoid the formation of an internal electric field due to the build-up of charge. The process continues until the voltage/current limits supplied by the external power source are met. If the current limit is made sufficiently high (about μA), a conductive silver bridge can be formed (electro-deposited) which connects (or bridges) the electrodes **201**, **202**. Once this conduction path is formed, no further power is required to maintain it. To reverse this process, the electro deposit is made positive by switching the polarity of the voltage with respect to the original oxidizable electrode, causing the dissolution of the metal bridge. During the dissolution of the electro deposit, the balance is maintained by deposition of metal back onto the oxidizable electrode **201**. Once the electro deposit has been completely dissolved, the process terminates. For this process to occur, a metal ion-rich anode is required to induce appreciable ion current flow. Further, to be reversible, the opposing electrode (cathode) must be made electrochemically inert (not oxidizable). A person having ordinary skill in the art will appreciate that this is merely example and other materials may be used for the electrodes, such as those described herein.

The measured insertion loss ("on"), isolation ("off") and power transfer curves for the nanoionics-based switch **100** (or **100**A, **100**B, **100**C, **200**A, **200**B hereinafter "the switch **100**") are shown in FIGS. **6** and **7**, respectively. The switch **100** operates by applying a voltage and a current, such as on the order of μA to mA, and forming a low loss conductive pathway in the base material **179** between the two electrodes **101**, **102** (or **105**, **106**, **121**, **122**, **151**, **152**, **201**, **201**, hereinafter "the electrodes **101**, **102**"). See FIG. **2**D which illustrates the actual growth of the electrodeposits. This process occurs via an oxidation-reduction reaction. Oxidation occurs at the oxidizable electrode **101** to form ions that can migrate into the chalcogenide glass (or the base material **179**) while electrons are simultaneously injected at the opposite inert electrode **102**. This combination ionic-electronic process induces a reduction reaction within the base material **179** to form a substance capable of "growing" across the gap **104** (or **109**, **123**, **153**, hereinafter "the gap **104**") between the electrodes **101**, **102**. For example, the oxidizable electrode **101** can be metal and may be oxidized to form metallic ions that migrate into the base material **179**, such as chalcogenide glass. The reduction reaction within the base material **179** can form metal which responds to an electric field and "grows" across the gap **104** until the power limit applied is reached. No further power is then required to maintain the "on" state of the switch **100**. To reverse this process, the polarity of the applied voltage is reversed and the electrochemically grown metal within the gap **104** oxidizes, returning the switch **100** to the "off" state.

FIG. **1**D is a schematic cross-sectional view of a nano-ionic switch **100**D having the substrate **103**, the base material **179**, and the electrodes **101**, **102**. A switch member **187** is electrically connected to a direct current voltage source **183** and the inert electrode **102**. The oxidizable electrode **101** is connected to the direct current voltage source **183** opposite the switch member **187**. A gap **109** is formed between the electrodes **101**, **102**. FIG. **1**D represents a simple positive bias of the oxidizable electrode **101** with respect to the negative bias of the inert electrode **102**. FIG. **1**E is a schematic cross-sectional view **100**E of the substrate **103**, the base material **179**, the electrodes **101**, **102** and a direct current voltage source **186**A. FIG. **1**E indicates a positive bias from a voltage source **186**A being controlled by the switch member **187**A and applied to the inert electrode **102** with the potential of the negative portion of the source being tied to the oxidizable electrode **101**. Applying the voltage potential of voltage source **183** across the electrodes **101** and **102** causes electrodeposits to "grow" across the gap **109** at the rate set forth by the following equations, where v_{Ag} is the speed of growth in the base material **179** (or solid electrolyte) and "d" is the size of the gap. The speed of growth, v_{Ag}, and the switch time, t_{switch}, and resistance, R, of the gap **109** are approximately as follows:

v_{Ag}=1 nm/ns

$t_{switch}=d/v_{Ag}$ where d=10 μm, then t_{switch}=10 μs

$R=L/\sigma_m$, for silver σ_m the conductivity is 50×10^5 S/m, and for electrodeposit in gap 10 μm long, 10 μm wide and 50 nm high, is, 1Ω.

Referring to FIG. **1**D, for a 10 μm gap, the growth of the electrodeposit will take approximately 10 μs. After approximately 10 μs, the switch member **187** may be opened and no further power is required to maintain conductivity of the switch **100**D. FIG. **2**C is a microphotograph **200**C of a portion of the oxidizable electrode **201**, the inert electrode **202** and the gap **204** of the nanoionic switch **100** schematically set forth in FIG. **1** in the "on" state (switch is closed). FIG. **2**D is an atomic force microscopic image **200**D of a portion of the gap **204** of the nanoionic switch **100** of FIG. **1** with the switch in the "on" state (switch is closed). Filaments **205** are shown in the microphotographs traversing the gap **204** in many areas. The filaments **205** are the growth of metal from the oxidizable electrode **201** as illustrated in FIGS. **2**C and **2**D. In the color micrographs submitted with this disclosure, FIG. **2**C shows the filaments as pinkish in some areas and as darker in other areas. FIG. **2**D is the atomic force microscope image, and this image illustrates raised structure referred to as dendrites which appears as ridges and cloud-shaped structures. These filaments and ridges (dendrites) shown in FIGS. **2**C and **2**D are conductive pathways that are established upon the application of bias potential with positive bias applied to the oxidizable electrode **201** and with negative bias applied to the inert electrode **202**.

It is instructive to compare FIG. **2**A ("off" state microphotograph of the switch **100**) with FIG. **2**C ("on" state microphotograph of the switch **100**) and also to compare FIG. **2**B ("off" state atomic force image of the switch) with FIG. **2**D ("on" state atomic force image of the switch). FIG. **2**A is a microphotograph **200**A of a portion of the oxidizable electrode **201**, the inert electrode **202** and the gap **204** of the nanoionic switch **100** of FIG. **1** depicting the switch **100** in the "off" state (switch is open). FIG. **2**B is an atomic force microscopic image **200**B of a portion of the gap **204** and of the electrodes **201**, **202** of the switch **100** of FIGS. **1** (and **2**A) with the switch in the "off" states (switch is open). The gap **204** which is illustrated in the microphotographs as the darker area in black and white and in the darker reddish areas of the color microphotographs filed with this patent application is the ternary or solid electrolyte which includes the silver-germanium-selenium ternary. Germanium and Selenium are a binary into which silver is photodissolved creating a ternary as described herein.

As illustrated in FIG. **1**E, the switch **100**E may be returned to its "off" state by applying positive voltage from the source **186**A to the inert electrode **102** and by applying (throwing the switch member **187**A) the negative voltage from the source voltage **186**A for a sufficient time as dictated by the switching time as stated above. The switch member **187**A controls the application of reverse bias in FIG. **1**E.

FIG. **1**F is a schematic cross-sectional view **100**F of the substrate **103**, the base material (or solid electrolyte) **179**, the electrodes **101**, **102**, a switch member **187**B and an alternating current power supply **184** applied across the electrodes **101**, **102**. Referring to FIG. **1**F, a sinusoidal voltage source **184** may be applied (controlled by the switch member **187**B) to the electrodes **101**, **102**. Once the growth of metal has been established across the gap **109** and/or in the base material (or ternary) **179**, the switch member **187** can be opened and no further power is necessary. The switch **100** disclosed herein is a nonvolatile switch meaning once the metal has filled the gap **104**, then no further power is required to maintain the switch **100** in the closed position. A sinusoidal signal may be passed through the switch **100** at frequencies greater than the switching time and/or having an rms (root mean square) voltage below the voltage necessary to activate the switch **100**.

The switch **100** exhibits switching times according to the equation above and the switching times are on the order of less than 1-10 microseconds (μs) which equate to frequencies of 1 MHz to 100 kHz. See FIG. **8**. However, the duration and voltage of the half-cycle of those frequencies should be considered lest the switch **100** might actuate inappropriately. Therefore, for a sinusoidal waveform being passed through the switch **100**, the specific switch time for the particular switch should be considered and the root mean square voltage (hereinafter "rms voltage") for the half cycle should be less than the actuation voltage (closing the switch). In addition, the rms voltage for the negative half cycle should be less than the reset actuation voltage (opening the switch). For example, if the period of the incoming signal being passed through the nonvolatile switch is too long (the frequency is too low), then the switch **100** could change states and reset with each cycle of the input signal.

FIG. **3** is a cross-sectional view **300** taken along the lines **3-3** of FIG. **2** illustrating the substrate **103**, the base material (or ternary) **179**, the oxidizable electrode **107** and the inert electrode **108**. FIG. **3**A is cross-sectional view **300**A similar to FIG. **3** along with a passivation layer **111** above the electrodes **107**, **108** and traversing the gap **109** between the electrodes **107**, **108**. FIG. **3**A also illustrates the substrate **103**, the base material (or ternary) **179**, the metallic plated **106**A oxidizable electrode **107** and the metallic plated **106**A inert electrode **108**. The metallic plating **106**A can be added to the electrodes **107**, **108** to reduce ohmic contact losses.

The electrodes **107**, **108** can be dissimilar metals and can be plated to a thickness of, for example, 1.5-2.0 μm. As a non-limiting example, the base material (or ternary) **179** may have a thickness of approximately 500 μm as illustrated in FIG. **3**A, and the gap **109** may be approximately 10 μm as measured between the electrodes **107**, **108**. Of course, those having ordinary skill in the art will appreciate that other separation distances may be utilized, such as those in the range of 0.1 to 500 μm.

Within the gap **109**, a thin film (for example, about 100 nm) of silver-saturated $GeSe_2$ glass (as an example) can be deposited which represents the active area of the switch **100**. Alternatively, the silver saturated glass is deposited first over a wide area of the substrate **103** and then the electrodes **107**, **108** are deposited thereover. A transmission line can taper to a higher impedance (narrowed width, 10 μm) transmission line toward the gap **109**. The tapering effect can help to reduce capacitive coupling in the switch in the "off" state, but remains the primary source of loss in the "on" state (due to a higher resistance because of a narrower channel). The passivation layer **111** can be silicon dioxide positioned atop the "active" area to provide protection.

By way of example, to operate the switch **100**, a voltage of nominally 0.3-1V and a current limit of 10 mA were used. The resistance in the "on" state was approximately 10Ω.

Higher voltages induced faster growth rates, whereas higher current limits reduced the overall resistive loss of the electrochemically grown metal, but resulted in higher power requirements to operate the switch **100**.

The application of a positive voltage relative to the inert electrode **108** induces metallic growth and enables the device to be turned "on." Reversing polarity of the applied voltage removes the electrochemically grown silver and forces the device into the "off" state. FIG. **2**C is a microphotograph of the conductive metallic pathways that form when the device is "on". FIG. **2**D is an atomic force microscope image after the switch **100** has been closed and shows that much of the metallic growth occurs on the surface of the thin film of the ternary **179**.

To measure the microwave performance of the switch **100**, test samples were individually diced and mounted onto a brass mounting fixture. The circuit was connected to an Agilent E8361A Vector Network Analyzer in order to measure "on" state insertion loss and "off" state isolation. An Agilent E3646A DC Power Supply was utilized to provide the necessary voltage/current to change the state of the device (nominally 1V/10 mA ("on") and −1V/10 mA ("off")). A plot of these results is shown in FIG. **7** for the nanoionic switch **100**. The insertion loss of the switch in the "off" state is better than −0.5 dB over the DC (zero hertz) to 6 GHz range (commercial ISM Band), while the isolation in the "off" state is better than −35 dB. A −0.5 dB insertion loss equates to approximately a 5.9% energy loss with the switch inserted in the circuit meaning that the switch is closed. Similarly, a −35 dB isolation loss equates to approximately 1.8% energy loss with the switch open. These measured results are comparable to MEMS and solid state-based RF switch performance in the same frequency range as indicated in FIG. **8**.

Power measurements were performed using an Anritsu ML2437A power meter and Anritsu MG3691B signal generator. The switch **100** was mounted on the same brass mounting fixture while various frequencies (500 MHZ-4 GHz) of varying power were fed into the switch **100**. Attenuation pads at the input and output to the switch **100** were used to reduce signal reflection within the system. The results are illustrated in FIG. **7** by the dark linear line. All of the frequencies 500 M Hz, 1 G Hz, 2 G Hz, 3 G Hz and 4 G Hz) were within the width of the dark line of the plot which indicates linearity over a wide band of frequencies.

FIG. **4** is schematic top view of a first example of nanoionic capacitor **400**. FIG. **4**A is a schematic cross-sectional view **400**A of the nanoionic capacitor **400** of FIG. **4** illustrating electrodes **407** (anode, oxidizable electrode) and **406** (cathode, inert). As described above, direct current voltage is applied to the oxidizable electrode **407** and the inert electrode **406** via the direct current voltage source **186** for a period of time to grow (electrodeposit) the metal, such as silver, from the oxidizable electrode **407** to the inert electrode **406** across gap **109**A, thus closing the switch **100**. Once the switch member **187** is closed then the nanoionic capacitor **400** is formed between conductive plate **405** and the plate formed by the electrodeposit which has filled the gap **109**A. See FIG. **2**D for an illustration of the switch **100** with the electrodeposit "grown" across the gap **204**. Once the electrodeposit has been formed, it acts as a capacitor plate as does silver anode **407**. The capacitor **400** can then be used for any function normally performed by capacitors such as in band pass filters, coupling capacitors and the like.

FIG. **4**B is a top schematic view of a plate (lower plate) **400**B that can be utilized in the capacitor **400**. The lower plate **400**B includes transmission lines **420**, **440** and a narrower section **430**. The narrowed section **430** of plate **400**B can have the same shape as the electrodeposited plate in the gap **109**. In this example, the nanoionic switch **100** of FIG. **3** can be used with the lower plate **400**B depicted in FIG. **4**B and can be separated by a dielectric. FIG. **4**C is a top schematic view of one of the two capacitor plates, namely an upper plate **400**C that may be used in this example of the nanoionic capacitor **400**. FIG. **4**C illustrates the oxidizable electrode **107** separated by the gap **109** from the inert electrode **108**. FIG. **4**D is a top schematic view **400**D of the plates **400**B, **400**C (of FIGS. **4**B and **4**C) illustrated in an overlapping position crossing each other in an orthogonal relationship. FIG. **4**E is a cross-sectional view **400**E of the capacitor taken along the lines **4**E-**4**E of FIG. **4**D illustrating the upper plate **400**C (formed from the growth of the electrodeposit (not shown)) and the lower plate **400**B. Shoulders **431**, **432** are illustrated in FIGS. **4**D and **4**E and the shoulders **431**, **432** represent the taper of the lower plate **400**B of the capacitor **400**. When the electrodeposit is grown two plates exist, the first plate being the electrodeposit and the second plate being the narrow section **430** of the lower plate **400**B. It should be noted that the plates **400**B, **400**C of the example of FIGS. **4**B-**4**E may be rectangular in cross-section and/or similarly shaped. Further, it should be noted that FIG. **4**C can be similar in shape to the profiles illustrated in FIG. **2** and in FIG. **1**A. As indicated herein the shape of the wider portions of the conductors **420**, **440** and their tapered (unnumbered) and narrow portion **430** can be similar to the wider portions **105**, **106**, the tapered portions **107**A, **108**A and the narrow portions **107**, **108**. See FIGS. **4**B-**4**E and FIGS. **1**A and **2**. The plates just described are separated by a dielectric **490**. No dielectric may be required if the substrate **103** is a dielectric and the metallic doping of the ternary that does not extend therethrough is a dielectric.

FIG. **6** is a plot **600** of insertion loss (switch closed or "on") and the isolation (switch open or "off") for frequencies between 1 and 6 GHz. FIG. **7** is a generalized plot **700** of power in versus power out for four frequencies (500 MHZ, 1 GHz, 2 GHz and 4 GHz). From FIG. **7**, it can be seen that devices typically demonstrated linearity over the range of measured power from −20 dBm to +20 dBm, with device breakdown typically occurring at about 400-500 mW. Further, no change is evident in the power transfer curve at different frequencies of operation, demonstrating the device's wide bandwidth operation potential.

The speed of operation of the nanoionic switch **100** can be a function of the distance the electrodeposit has to traverse. Or, put another way, the electrodeposit has to grow a certain distance within the ternary or on top of the ternary (or base material **179**). That is, the wider the gap **109** between the electrodes **101**, **102**, the longer the response time of the switch **100**. Although the switching speed was not directly measured, results inferred from M. N. Kozicki, M. Yun, L. Hilt, A. Singh, "Application of programmable resistance changes in metal-doped chalcogenides," Proceedings of the 1999 Symposium on Solid State Ionic Devices, Electrochemical Society Proceeding, Vol. 99-13, p. 298 (1999), indicate that the electrodeposition rate of silver within a chalcogenide glass occurs at a velocity of approximately 1 nm/ns. Therefore, for a 10 μm gap, a switching speed of around 10 μs is expected. Obviously the smaller the gap size, the faster the switch operation, but other considerations such as "off" state isolation limit the optimization of speed, at least for a coplanar-type structure.

FIG. **5**A is a schematic **500**A of a single-pole, "N" throw nanoionic switch. In FIG. **5**A, "P" represents the pole or anode and T**1** through Tn represents "N" possible throws.

Since the active switching element is comprised of simply a thin film area, the addition of extra electrodes (ports or throws "N") in contact with the active area makes possible the creation of SPNT (single-pole-n-throw-switches), as shown in the diagram of FIG. 5A. Application of the necessary voltage across the electrodes results in a conductive pathway which can be formed/dissolved amongst one of several different paths limited only by available space and maximum coupling level requirements. Further, the ability to deposit "vias" of this nanoionic material allows for the formation of multilayer control circuits. "Vias" are the through-hole paths to other surfaces of an integrated circuit having multiple layers. Use of a switching network in a horizontal and a vertical fashion has the advantage of compacting circuit footprints and reducing overall circuit losses. The disclosure of the nanoionic switch **100** herein represents an unprecedented ease of integration.

FIG. **5** illustrates a potential SP5T nanoionic switch **500**, showing multiple horizontal, as well as vertical, switching paths. One such application for the switch **500** can be in low-loss phased array technology. For conventional discrete phase shifters based on a solid state or MEMS approach, approximately 2N switches is required for an N-bit phase shifter, with 2-3 control lines per switch, contributing to the overall loss and complexity of the circuit. Advantageously, implementation of the nanoionic topology described herein results in an N-bit phase shifter with only one nanoionic switch and N+2 control lines. A control line may be required for each of the N-bits. Additionally, a control line may be necessary to switch positive potential to the pole (oxidizable electrode) and another control line is needed to switch negative potential for a bus interconnected with the phase shifters (inert electrode). This example discloses the structure necessary for minimizing losses as the insertion loss of each of the phases is low and the line losses (and not switch losses) will be the primary contributor to total phase shifter loss.

Referring to FIG. **5**, the SP5T nanoionic switch **500** is formed as first throw **501**, second throw **502**, third throw **503**, fourth throw **504**, and fifth throw **505**. Each of these throws **501**, **502**, **503**, **504** can be a nanoionic switch wherein an electrodeposit is grown over and through respective horizontal or vertical gaps. Each switch operates between (anode, oxidizable pole) **590** and a first delay line **591**, a second delay line **592**, a third delay line **593**, a fourth delay line **594**, and a fifth delay line **595**.

FIG. **9** illustrates a system **900** that may be utilized with a nano-ionic switch as previously mentioned herein, such as the nanoionic switch **100** (or **100**A, **100**B, **100**C, **200**A, **200**B, **500**, together hereinafter "the switch **100**"). As shown in FIG. **9**, the switch **100** may be positioned between a first rectenna module **920** and a second rectenna module **930**. As mentioned, the switch **100** may comprise the elements of the switch **100** as set forth herein, including having the oxidizable electrode **101** and the inert electrode **102** positioned on chalcogenide glass such that the gap **109** exists between the oxidizable electrode **101** and the inert electrode **102**. A conductive bridge can be formed at the gap **109** between the electrodes **101**, **102** upon activation application of voltage on the switch **100**.

Advantageously, the embodiment of FIG. **9** may be used without an active voltage source. For example, no on-board power may be required to operate the switch **100**. Instead, the rectenna modules **920**, **930** may be connected to the switch **100** and permit control of the switch **100**, such as closing or opening the switch **100**, from a location remote from the switch **100** and/or the rectenna modules **920**, **930**. In an embodiment, the switch **100** functions by way of a wireless, contact-less induced change of polarity on the electrodes **101**, **102** to enable either a highly conductive or a highly resistive path between the electrodes of the switch **100**.

For example, each of the rectenna modules **920**, **930** may comprise one or more components to receive a signal, such as an antenna, and one or more transducers. In an embodiment, the rectenna modules **920**, **930** comprise a rectifying element, such as a nonlinear rectifying element or nonlinear rectifier. The components and/or transducers of the rectenna modules **920**, **930** may be electrically connected to the nono-ionic switch **100**. The rectenna modules **920**, **930** may have one or more devices and/or features capable of receiving a first type or frequency of energy and converting or transforming the first type of energy to electrical energy to control the switch **100**. In an embodiment, the rectenna modules **920**, **930** may receive microwave energy or a radio frequency signal (hereinafter "RF signal"), such as radio frequency energy, and convert the microwave energy or the RF signal to electrical current, such as alternating electrical current or direct electrical current.

For example, the first rectenna module **920** may have a first antenna **922**, a first diode **924**, and a first filter **926**. The second rectenna module **930** may have a second antenna **932**, a second diode **934**, and a second filter **936**. The first filter **926** may be positioned such that the first filter **926** is positioned between one of the electrodes **101**, **102** of the switch **100** and the first diode **924**. The second filter **936** may be positioned between one of the electrodes **101**, **102** of the switch **100** and the second diode **934**. The filters **926**, **936** may be low pass filters configured to attenuate or suppress high-frequency signals received therein. The filters **926**, **936** may be capacitive or inductive low pass filter as non-limiting examples. A person having ordinary skill in the art will appreciate the filters **926**, **936** may be configured based on application of the switch **100** and/or the rectenna modules **920**, **930**.

The antennas **922**, **932** may be any type of antennas to receive the first type or frequency of energy. For example, in order to receive the RF signal, the antennas **922**, **932** may be microwave antennas, broadband antennas, large antenna arrays, circular polarized antennas, microstrip antennas, such as microstrip square-patch antennas, or any other type of antenna capable of receiving the first type of energy, such as the RF signal. The broadband antenna may enable relatively high frequency RF signals to be received while an antenna array can increase incident power delivered to the first diode **924** or the second diode **934**, respectively. In an exemplary embodiment, the antennas **922**, **932** may be a circular antenna, such as a microstrip circular-sector antenna. The circular antenna can offer power reception with less polarization mismatch. For example, the circular antenna may suppress radiations of the second and third harmonics such that a filter, such as the filters **926**, **936**, between the first antenna **922** or the second antenna **932**, and the first diode **924** or the second diode **934**, may not be necessary.

The first diode **924** and the second diode **934** may comprise a diode, such as a Schottky diode, an IMPact ionization Avalanche Transit-Time diode ("IMPATT diode") or other type of diode that will be appreciated by those having ordinary skill in the art. As an example, the first diode **924** and the second diode **934** may be any device having an asymmetric transfer characteristic with low resistance to current flow in one direction and a high resistance to current flow in the other direction.

In use, a first wireless signal, such as the RF signal, may be transmitted from a location remote from the rectenna modules **920**, **930**. The first wireless signal can be received at the first rectenna module **920**, such as by the first antenna **922**. The first antenna **922** can be electrically connected to the first diode **924** and the first filter **926** to convert the RF signal into electrical energy and to apply a first bias based on the RF signal across the nano-ionic switch **100**. The first bias can change a state of the nano-ionic switch **100** from a first state to a second state, such as from an "off" state to an "on" state. For example, as shown in FIGS. **1** and **2**, the oxidizable electrode **101** is made positive (anode) with respect to the inert electrode **102** if sufficient bias is applied.

As an example, the oxidizable electrode **101** is oxidized to form an excess of metal ions within the chalcogenide base glass (or base material **179**). The applied field causes the positive metal ions to flow toward the inert electrode **102** through the coordinated hopping mechanism described above. At the inert electrode **102**, a reduction reaction can occur by electrodepositing the metal and eventually forming a conductive bridge across the gap **109** between the electrodes **101**, **102**. The switch **100** can now be considered to be in the "on" state and can be maintained at this state with little or no continued or additional voltage. For example, without further electrical power and without further or continued receipt of the first wireless signal, the switch **100** can remain in the "on" state.

In order to revert or change the state of the switch **100** from the "on" state to the "off" state, a second wireless signal can be transmitted from a location remote from the rectenna modules **920**, **930** to, for example, the second rectenna module **930**. The second wireless signal can be received at the second rectenna module **930**, such as by the second antenna **932**. The second wireless signal can be at a different frequency from the first wireless signal. Accordingly, the first antenna **922** can be tuned to receive signals within a first frequency range, and the second antenna **932** can be tuned to receive signals within a second frequency range, different than the first frequency range. The second antenna **932** can be electrically connected to the second diode **934** and the second filter **936** to convert the RF signal into electrical energy and to apply a second bias based on the RF signal across the nano-ionic switch **100**. The second bias can change a state of the nano-ionic switch **100** from the second state to the first state, such as from an "on" state to an "off" state. The second bias may be reversed, negative or opposite with respect to the first bias. For example, as shown in FIGS. **1** and **2**, the electrochemically grown metal within the gap **109** oxidizes, returning the switch **100** to the "off" state. For example, the oxidizable electrode **101**, **201** is made positive with respect to the inert electrode **102**, **202** until the gap **109** again is formed between the electrodes **101**, **102**.

FIG. **10** illustrates an embodiment of a rectenna module **1000** which may be utilized in the embodiment of FIG. **9**. In an embodiment, the rectenna module **1000** may replace the rectenna modules **920**, **930**. The rectenna module **1000** may comprise one or more components to receive a signal, such as an antenna, and one or more transducers. In an embodiment, the rectenna module **1000** can comprise a rectifying element, such as a diode **1002**. The components of the rectenna module **1000** may be electrically connected to the nono-ionic switch **100**. The rectenna module **1000** may have one or more devices and/or features capable of receiving a first type or frequency of energy and converting or transforming the first type of energy to electrical energy to control the switch **100** (shown in FIG. **9**). In an embodiment, the rectenna module **1000** may receive the RF signal and convert the RF signal to electrical current, such as alternating electrical current or direct electrical current. The rectenna module **1000** may have an antenna **1022**, the diode **1002** and a filter **1026**. The filter **1026** may be positioned such that the filter **1026** is positioned between one of the electrodes of the switch **100** and the diode **1002**. The filter **1026** may be low press filters configured to attenuate or suppress high-frequency signals received therein.

In use, the rectenna module **1000** may receive the RF signal, such as at the antenna **1022**, at a first frequency to apply a first bias based on the RF signal across the nano-ionic switch **100**. The first bias can change a state of the nano-ionic switch **100** from a first state to a second state, such as from an "off" state to an "on" state. For example, as shown in FIGS. **1** and **2**, the oxidizable electrode **101**, **201** is made positive (anode) with respect to the inert electrode **102**, **202** if sufficient bias is applied. As an example, the oxidizable electrode **101** is oxidized to form an excess of metal ions within the chalcogenide base glass (or base material **179**). The applied field causes the positive metal ions to flow toward the inert electrode **102**, **202** through the coordinated hopping mechanism described above. At the inert electrode **102**, **202**, a reduction reaction occurs by injecting electrons to re-form the metal and eventually form a conductive bridge across the gap **109** between the electrodes **101**, **102**. The switch **100** can now be considered to be in the "on" state and can be maintained at this state with little or no continued or additional voltage. For example, without further electrical power and without further or continued receipt of the first wireless signal, the switch **100** can remain in the "on" state.

In order to revert or change the state of the switch **100** from the "on" state to the "off" state, the first wireless signal may be sent again to the rectenna module **1000**. Alternatively, the second wireless signal may be sent to the rectenna module **1000** comprising a microwave or the RF signal at a frequency different than the first wireless signal. In either instance, the first wireless signal or the second wireless signal can be transmitted from a location remote from the rectenna module **1000** and the antenna **1022**. Advantageously, the rectenna module **1000** may include a polarity switch **1050** electrically connected to the antenna **1022**, the diode **1002** and the filter **1026** as shown in FIG. **10**. The polarity switch **1050** can be configured to control the bias across the nano-ionic switch **100**. As an example, the polarity switch **1050** may apply a second bias that is a reverse or opposite of the first bias upon the antenna **1022** receiving the first wireless signal again (e.g. a second time or twice in a row) or receiving the second wireless signal. As mentioned above, the second bias can change the state of the switch **100**, such as change a state of the switch from an "on" state to an "off" state. The second bias can, for example, as shown in FIGS. **1** and **2**, cause oxidize the electrochemically grown metal within the gap **109**, returning the switch **100** to the "off" state. The oxidizable electrode **101**, **201** can be made positive with respect to the inert electrode **102**, **202** until the gap **104** again is formed between the electrodes **101**, **102**.

The polarity switch **1050**, therefore, permits use of the nano-ionic switch **100** with only one rectenna module **1000**, in at least an embodiment. At a minimum, the polarity switch **1050** permits control of the switch **100** to move from an "on" state to an "off" state and back again with only the use of a single rectenna module **1000**. The polarity switch **1050** may be any device or combination of devices to permit a first bias and a second bias, the second bias being opposite the first bias. Accordingly, the polarity switch **1050** is configured to apply a positive bias to the oxidizable electrode **101** in certain instances as set forth herein, and the polarity switch **1050** can apply a negative bias on the oxidizable electrode **101** in other instances. For example, the polarity switch **1050** may apply a positive bias on the oxidizable electrode **101** upon receipt of the first wireless signal, and the polarity switch **1050** may apply a negative bias on the oxidizable electrode **101** upon receipt of the first wireless signal again or receipt of the second wireless signal at the antenna **1022**.

Those skilled in the art will readily recognize that the invention has been set forth by way of examples only and that changes may be made to the invention without departing from the spirit and scope of the appended claims.

The invention claimed is:

1. An apparatus comprising:

a nanoionic switch having a first state and a second state;

at least one rectenna module, comprising an antenna and a rectifier, coupled to the nanoionic switch; and

wherein the rectenna module permits operation of the nanoionic switch without onboard power.

2. The apparatus according to claim **1**, wherein a signal at a first frequency or a signal at a second frequency changes the state of the nanoionic switch from the first state to the second state.

3. The apparatus according to claim **2**, wherein the rectenna module receives and converts a signal at a first frequency or a signal at a second frequency into electrical charges.

4. The apparatus according to claim **3**, wherein the electrical charges change the nanoionic switch from a first state to a second state.

5. The apparatus according to claim **1**, wherein the nanoionic switch further comprises an oxidizable electrode and an inert electrode with a gap between the oxidizable electrode and the inert electrode.

6. The apparatus according to claim **5**, wherein the inert electrode and the oxidizable electrode are positioned on chalcogenide glass.

7. The apparatus according to claim **6**, wherein a conductive bridge is formed at the gap between the oxidizable electrode and the inert electrode, without any power source.

8. The apparatus according to claim **7**, wherein electrical current is directed to the oxidizable electrode to change the state of the nanoionic switch.

* * * * *